2002

Parametric and sensitivity analysis of a vibratory automobile model

Kanika Nicole Vessel
Louisiana State University and Agricultural and Mechanical College, kmixon1@lsu.edu

PARAMETRIC AND SENSITIVITY ANALYSIS OF A VIBRATORY AUTOMOBILE MODEL

A Thesis

Submitted to the Graduate Faculty of the
Louisiana State University and
Agricultural and Mechanical College
in partial fulfillment of the
requirements for the degree of
Master of Science in Mechanical Engineering

in

The Department of Mechanical Engineering

by

Kanika Nicole Vessel
B.S. in Mechanical Engineering
Southern University and A & M College, 1999

May 2002

DEDICATION

To my husband Bradley D. Vessel,
my parents Theophilus and Nordica Mixon, Jr., my
grandparents Robert and Mary Pierce, my uncle
Eddie Pierce, my aunty Debra Morgan, and my
siblings, LaKenya, Keesha, Damon, Tecarai, and Eric

ACKNOWLEDGMENTS

First and foremost I would like to give thanks and all honor to God. Without Him I would not be where I am today.

I would like to acknowledge my major professor Dr. Su-Seng Pang for his continued guidance and support while making sure I stay focused. Thanks also go to Dr. Yitshak M. Ram and Dr. Lynn Lamotte for serving on the graduate committee and evaluating my thesis. Thanks to Dr. Yitshak M. Ram for serving as co-advisor on my graduate committee. Furthermore, I would like to thank Dr. Michael A. Stubblefield for his advise and support during this advanced degree program.

Thanks to my colleagues Akshay Nareshraj Singh and Kumar Vicram Singh for their intellectual input. Also, thanks to Salvador Cupe-Beecha, Mr. Ed Martin and Jim Layton, Jr. for their assistance in constructing the lab experiment.

Thanks to my friends Shani Allison, Caroline Stampley, Tameka Williamson, Kristian Johnson, Phaedra Bell, Shari Jones, and Thereza Shanklin for their continued support when times were tough. Thanks to the Pierce, Carter, Mixon and Williams family for their continued support.

My gratitude goes to my uncle Eddie Pierce for being like a father to me and to my aunty Debra Morgan who has always been there for me. Special thanks to my mom Nordica Mixon for her faith, guidance, love, support, strength as single parent, and for being one of my very best friends as well. Thanks to my dad Theophilus Mixon, Jr. for being stern when I needed discipline, but also for being my friend when I needed one. Last but certainly not least, my husband. Thanks for all your love, support, strength and faith when I needed it.

Thanks to NSF/Interactive Graduate Education Research Training and NASA/LaSpace for their financial support to make this possible.

TABLE OF CONTENTS

LIST OF TABLES

LIST OF FIGURES

ABSTRACT

Vibration response is an important aspect of any engineering problem. This thesis deals with developing a method to obtain the vibration, parametric and sensitivity of an automobile analyzed as a 2-DOF rigid body system with damping. The focus of the vibration analysis is to obtain the poles, eigenvectors, and natural frequencies of the system. The parametric analysis gave information on how the natural frequency is affected when one of the parameters is perturbed. Information about how much the system is affected by the change in one parameter is what is obtained from the sensitivity analysis. The theoretical solution contained in this report uses the parameters of a 2002 Honda CR-V to give a general idea of how an automobile should respond when analyzed as a two degree of freedom rigid body.

An experiment was designed to implement the theory in practical applications. Modal testing was applied to extract the natural frequencies in order to characterize the system. From the experiment, the parametric analysis produced results that resulted in error of 5.8-10.8%. This error is small and it may seem the experiment is a good design, but that error caused an even greater amount of error in the sensitivity results. In that analysis, the stiffness produced the best results, resulting in 0% error. However, the error for the sensitivity on the mass resulted in 28.09-54.0% for the first eigenvalue and 18.94-24.76% for the second eigenvalue. This high error could be due to the fact that the mass is a sensitive parameter. For the most part, fairly accurate results have been produced from the developed theory. Some work still needs to be done with the sensitivity to get better results. These results also prove that this theory can serve as a vital tool in developing practical solutions to vibration control problems.

CHAPTER 1: INTRODUCTION

1.1 General Introduction

Vibration, which occurs in most machines, structures, and mechanical components, can be desirable and undesirable. Vibrations on the strings of a harp are desirable because it produces a beautiful sound. However, vibration in a vehicle is very undesirable because it can cause discomfort to the passengers in the vehicle. Vibration is undesirable, not only because of the unpleasant motion, the noise and the dynamic stresses, which may lead to fatigue and failure of the structure, but also because of the energy losses and the reduction in performance which accompany the vibrations. Vibration analysis should be carried out as an inherent part of the design because of the devastating effects, which unwanted vibrations could have on machines and structures. Modifications can most easily be made in an effort to eliminate vibration, when necessary or to reduce it as much as possible.

There are several classifications of vibration, free and forced, undamped and damped, and linear and nonlinear vibration. Free vibration is when a system, after an initial disturbance, is left to vibrate on its own. No external force acts on the system. If a system is subjected to an external force, the resulting vibration is known as forced vibration. If the frequency of the external force coincides with one of the natural frequencies of the system, a condition known as resonance occurs, and the system undergoes dangerously large oscillations. Undamped vibration is when no energy is lost or dissipated in friction or other resistance during oscillations. On the other hand, when energy is lost in this way, it is known as damped vibration. Linear vibration is when all the variable forces are directly proportional to the displacement, or to the derivatives of

the displacement, with respect to time. On the other hand, if any of the variable forces are not directly proportional to the displacement, or to its derivatives with respect to time nonlinear vibration occurs.

In vibration, a number of simplifying assumptions have to be made to model any real system. For example, a distributed mass may be considered as a lumped mass, or the effect of damping in the system may be neglected particularly if only resonant frequencies are sought, or a non-linear spring may be considered linear, or certain elements may be neglected altogether if their effect is likely to be small. Furthermore, the directions of motion of the mass elements are usually restrained to those of immediate interest to the analyst.

1.1.1 Vibration in Automotive Industry

An automobile is made up of many components. These components include suspension, engine and its components, chassis, transmission, braking, etc. and represent the many subsystems in a multi-degree of freedom analysis. Yet, for many of the more elementary analyses applied to it, all components move together. The type of analysis used depends on what component is being investigated. For example, under braking, the entire vehicle slows down as a unit; thus it can be represented as one lumped mass located at its center of gravity with appropriate mass and inertia properties. One mass is sufficient for acceleration, braking, and most turning analyses. For ride analysis, it is often necessary to treat the wheels as separate lumped masses. In that case, the lumped mass representing the body is the sprung mass, and the wheels are denoted as unsprung masses. The vehicle is treated as a mass concentrated at its center of gravity for single mass representation. The point mass at the center of gravity, with appropriate rotational

moments of inertia, is dynamically equivalent to the vehicle itself for all motions in which it is reasonable to assume the vehicle to be rigid.

1.1.2 Basis of this Research

Engineering students often understand the theories and principles concerning vibration by doing homework assignments or performing lab experiments. However, it is not simple to design an experiment to implement these simple principles. A simple thing as determining the spring force of a spring or the natural frequency of a simple system can be a difficult experiment to perform. With homework assignments it is easy to use the known equations and given information to solve the problem without much thought. The same goes for lab experiments, the setup is given and the procedure is followed without much thought as to why certain components are chosen.

All mechanical systems have natural frequencies. When analyzing these systems engineers sometimes apply rigid body dynamics. Rigid body dynamics has been used in many industries such as automotive, agricultural and aerospace. In industry, multi-degree of freedom (DOF) systems is used to obtain measurements and simulate movement under certain conditions. The purpose of a multi-DOF system is to represent the subsystems of the body. When simplifying a mechanical system in terms of a rigid body, it is necessary to determine the best method to do that. Take for instance the research of Chrstos in [1]. He was interested in vehicle parameters required for vehicle dynamics simulation and determined there are three categories used to develop the vehicle dynamics simulation. The three categories are low DOF linear models, nonlinear lumped parameter models, and multi-body dynamic models.

The sophistication of simulation developed has ranged from 2-DOF linear models used to study low severity vehicle behavior to complex multi-body formulations used to investigate limit handling performance and vehicle rollover. The usage of the 2-DOF models is only a technique to extract meaningful parameters from measured data. Evaluation methods using an unreasonable number of parameters have no purpose for the development of new cars or for comparison of similar cars since drivers' preference vary widely in various handling characteristics. Mimuro *et al*. showed this in their research in [2]. He was interested in parameter evaluation of vehicle dynamic performance. These engineers developed a Four Parameter Evaluation Method. The lateral transient response data was curve fitted with a 2-DOF model and the parameters are extracted. The four parameters were expressed in a rhombus to help recognize vehicle performance intuitively. "The area of the rhombus denotes vehicle handling potential, and the distortion denotes handling tendency. The key point of this method was making it possible to see the parameters that contradict each other at a glance [2]".

The use of rigid body dynamics in system analysis can assist in any objective the engineer is trying to obtain, it is like a stepping-stone in system analysis. The parameters of focus for this experiment are mass (m), stiffness (k), damping (c), and moment of inertia (J). Two types of vibration will be investigated, free and forced. For both types of vibration, the theoretical results will be compared to the experimental results. The automobile body or sprung mass has two vibrations that are of interest for this experiment, vertical (bounce) and pitch. Figure 1.1 shows these two modes of vibration. Bounce is the translational component of ride vibrations of the sprung mass in the direction of the vehicle z-axis. Pitch is the angular component of ride vibration of the

sprung mass about the vehicle y-axis. Therefore, the automobile will be investigated as a rigid body 2-DOF system with damping. In addition to the vibration analysis, a parametric and sensitivity analysis will be performed as well. The parametric analysis will look at how perturbations in one parameter affect the natural frequency. The sensitivity analysis will look at how sensitive a parameter is to change in one or several other parameters.

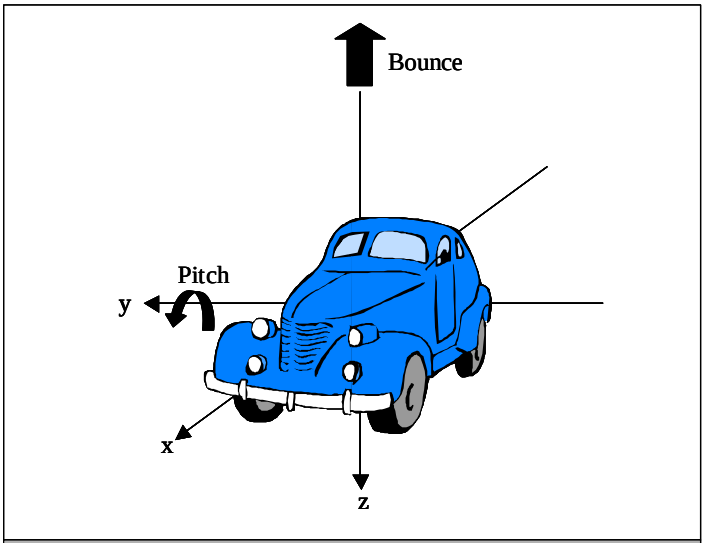

Figure 1.1: Bounce and pitch modes of vibration

1.2 Organization and Content of the Thesis

This thesis is divided into five sections, the structure and content of which are described below:

Section 1: Introduction (Chapter 1)

This section is a general introduction to the subject of vibration, parametric and sensitivity analysis, followed by a description of the organization and content of the thesis.

Section 2: Literature Review (Chapter 2)

This section is a literature review to investigate the effect of vibration on the automobile. This section reviews laboratory studies, which have investigated the effect of various parameters on automotive vibration. This section also consists of reviews that have investigated vibration on certain components of the automobile, as well as considering the automobile with certain degrees of freedom.

Section 3: Vibration, Parametric and Sensitivity Analysis (Chapter 3)

This section describes the theory for modeling free and forced vibration for a 2-DOF system with damping. Also included are the contributions of this experiment, which have not been previously investigated. The contributions are the parametric and sensitivity analysis for each parameter.

Section 4: Experimental Verification (Chapter 4)

Chapter 4 discusses the measurement process and the measurement instrument used for our experiment, as well as the experimental setup and results of the experiment.

Section 5: Conclusion and Recommendations (Chapter 5)

This section contains a summary of the principle conclusions reached on the basis of the literature review and subsequent experimental work. Included in this Chapter are recommendations for the direction of future research relating to vibration, parametric and sensitivity analysis.

CHAPTER 2: LITERATURE REVIEW

2.1 Introduction

The literature reviews that follow are to support the use of rigid body dynamic analysis. Using a 2-DOF model cannot only be used to see the frequencies of the system, but also to look at the effects of the suspension or the tires. Although only the bounce and pitch modes are being investigated, the automobile has other modes that can be investigated with a 2-DOF or a multi-DOF system. The literature on the tires is to show that using the stiffness, k, is justifiable in representing the tires. This chapter is divided into 4 sections: Vehicle System Modeling, Vehicle Structure Modes, Tire Properties and Vehicle Handling.

2.2 Vehicle System Modeling

Hovarth was interested in vehicle system modeling in order to provide a method of obtaining the dynamic response of the full vehicle when the dynamic characteristics of each component are known in [3]. A comparison was made between a Finite Element (FE) Approach and Modal Modeling. In the FE Approach, the mass and stiffness properties of the elements are representative of the properties of the real structure at the same location. The Modal Modeling method was based upon the fact that a structural component can be mathematically represented by its modal characteristic as well as by distributed mass and stiffness. In other words, modal models can be used as building blocks and coupled to mathematical models of the vehicle's other subsystems to simulate the behavior of the complete vehicle system. To obtain the best results for modal

modeling, the vehicle was divided into 4 subsystems. The modal modeling technique with 4-subsystem division was the best analysis technique because each subsystem assured the simplest approach necessary to obtain the required results. Therefore, the modal modeling technique could dramatically reduce the problem size and cost with no reduction in accuracy when compared to the FE approach.

Davis further investigated modal modeling by fitting the model to measure frequency responses in [4]. The foundation of modal modeling is the following principle: Vibrational response of any structure can be considered to be the sum of the responses of a set of coupled modes. The following 4 vehicle structure modes were examined: bounce, pitch, and 2 beaming modes. He concluded that the dynamic behavior of any structure can be completely simulated by a modal model. It is extremely important to predict how the vehicle structure interacts with its subsystems in order to obtain the total vehicle system. This is why modal models have become so useful.

Speckhart developed a 14-DOF mathematical model to analyze and predict the handling dynamics of a 4-wheel vehicle in [5]. There was no allowance for the deflection of any member; therefore, the vehicle was treated as an assembly of rigid masses when deriving the equations of motion. This study determined that small changes in the suspension design could make a noticeable difference in handling. The greatest sources of error in predicting the dynamic response were attributed to the uncertainty in determining the exact vehicle parameter and the performance of tires.

Simic and Petronijevic focused on the car body as an elastic structure in [6]. The modal vector, driving force, frequency and vibration characteristics of the elastic automobile structure determine the frequency response. They measured the vibrational

characteristics of the automobile body under the harmonic excitation forces at 5 points. The car body tested was freely supported on four springs. They realized the input signals could determine the actual vibration condition of a particular area of a car body. Possible helpful tools in the process of designing and developing the car body are information about the location of neutral lines and the shape of vibration modes.

Daberkow and Kreuzer investigated the integration of Solid Modeling Computer Aided Design (CAD) systems within a dynamic simulation environment in [7]. The modeling of a mechanical system by means of a multi-body system is based on the composition of rigid bodies, interconnected by joints, springs, dampers and actuators. The applied forces and torques on the rigid bodies are the force elements, which include springs, dampers and actuators acting in discrete attachment points. Joints with different kinematic properties have several effects on a mechanical system. They constrain the motion of the bodies of the system, determine the DOF of the multi-body system, and result in constraint forces and torques. In order to investigate a system without considering the geometric model, modeling method and the solid model construction of the CAD system in use, certain basic parameters are needed. The basic parameters needed for system dynamics investigations are mass, center of gravity and moments of inertia. The object-oriented classes and operations of this new approach are implemented in a system-independent multi-body modeling kernel library.

Huang and Chao used a quarter-car 2-DOF system to design and construct the concept of a four-wheel independent suspension to simulate the actions of an active vehicle suspension system in [8]. "A model-free fuzzy logic control algorithm is employed to design a controller for achieving vibration isolation [8]". To satisfy the

expectations of customers the requirements of ride comfort and driving performance are major development objectives of modern vehicles. The suspension system is an important factor to the ride comfort and driving capability. The active suspension consists of a spring, damper and actuator between the unsprung mass and sprung mass, where the sprung mass is considered as a rigid body. The fuzzy logic control algorithm suppressed the sprung mass vibration amplitude due to road variation. The vehicle suspension served to suppress the vibration amplitude of the vehicle body. This prevented the tire bouncing from the road surface owing to excessive tire deformation. In order to obtain ride comfort the spring and damping forces acting on the body must be compensated for. The control was used to compensate for these forces acting on the body. The experimental results showed that this control strategy has successfully reduced the oscillation amplitude of the vehicle body and improved the ride comfort.

Varadi *et al*. focused on a three-dimensional, computationally inexpensive vehicular model in [9]. In the past the vehicle's sprung mass is modeled as a rigid body, but in this research it is modeled as a nonlinearly deformable body. The theory of a Cosserat point was introduced to model three-dimensional deformable bodies with large deformations. When the theory of a Cosserat point is applied to vehicle dynamics, it is assumed that the sprung mass is deformable. "When applied to the sprung mass of a vehicle, it results in a mathematical model with relatively few degrees of freedom whose deformation can be used to explain the vents arising during a collision [9]". The methods used for rigid body models can be applied to the modeling of the unsprung mass of the vehicle and the tire/road interaction.

Zhang *et al*. investigated how two beam elements suspension/suspension models with rigid vehicle body representation and finite element tires were studied under proving ground conditions in [10]. The only difference between the two models was that one used flexible beam elements and the other used rigid beams. One of the obvious advantages of conducting rigid body dynamics analysis is timing. The main purpose was to show how suspension/suspension component flexibility and the consequence of small deformations in these components could affect the nonlinear dynamic analysis results. All the compliance/stiffness study results showed that there were differences between a suspension/suspension model with deformable components and one with only rigid body representation. In conclusion, the vehicle dynamic analysis results can be greatly affected by the type of suspension/suspension sub-system representation being used. The rigid vehicle body structure representation used in the present study had definitely some influence on the vehicle's dynamic characteristics and the simulation results.

2.3 Vehicle Structure Modes

Kawagoe *et al*. were interested in the influence of roll behavior on drivers evaluating handling performance in [11]. Prototype cars were used for the experiment. In the past, roll behavior of performance has been difficult to predict. In the past, indices for evaluating roll behavior has not correlated well with subjective evaluations. To improve roll behavior, the suspension properties of prototype cars had to be adjusted. The results suggested that vehicle pitch motion is closely related to the sensation of roll. In conclusion, pitch motion is an effective evaluation index for vehicle roll behavior and it correlates well with subjective evaluation results. Controlling pitch motion during roll to a lower mode at the front end relative to the rear is extremely important. This is the

key to acceptable roll behavior. Controlling of the pitch motion can be achieved by designing suitable roll center characteristics, nonlinear load changes and damping force coefficients.

Mehrabi *et al*. presented a parametric study of automated vehicles using the sensitivity theory in [12]. A sixth order dynamic model of an axisymmetric vehicle was developed to represent its 3-DOF motion in the lateral, yaw and roll modes. Important parameters of the vehicle are grouped into three separate vectors, inertia, stiffness and damping, and geometric-kinematic parameter, respectively. They investigated the effects of various parameters of automated vehicles on their dynamic performance. The results are useful for the design of both the mechanical structure of a vehicle and the its steering controller. Simulation results show that an increase in the mass of the vehicle significantly decreases the steady-state lateral velocity of the vehicle. Sprung mass and roll moment of inertia affect the roll transient response. Both transient and steady state responses of lateral velocity and yaw rate of the vehicle are sensitive to the cornering stiffness of the front tires. Stiffness and damping parameters had virtually no effect on the steady-state value of roll motion. Any increase in the forward vehicle speed increases the yaw rate considerably because it is the most sensitive state. In general, the vehicle parameters directly related to roll motion did not contribute significantly to the yaw and lateral motion. The most significant parameter affecting all the motion of the vehicle, especially yaw rate, was the forward speed of the vehicle. "The geometric-kinematic parameters were the most influential on the performance of the vehicle, especially the yaw rate [12]". Inertia parameters were the most influential when it came to the transient parts of the various responses.

El-Demerdash was interested in the performance of hydro-pneumatic limited bandwidth active suspension system using a half car model in [13]. The bounce and pitch motions for the sprung mass and 2 vertical DOF for the unsprung mass are considered. With the passive suspension systems it is difficult to achieve the conflicting requirements. This was because the principle vehicle dynamic modes: bounce, pitch and roll, ride comfort and maneuverability modes, must have different natural frequencies and damping for optimum suspension design. The half vehicle model is more convenient to study their influence on the interactions between the body bounce and pitch motions and to design the passive as well as the active suspension systems. The results showed that the system with wheelbase correlation provides 20% improvement in pitch acceleration and 18% reduction in the body vertical acceleration at the rear suspension connection compared with uncorrelated system. In comparison with passive system, there is 44% reduction in the pitch acceleration and 29% improvement in the body vertical acceleration at the rear suspension connection. This reduction in the pitch acceleration was useful to improve the ride comfort in the longitudinal direction. The advantage of the proposed suspension system was that its hydraulic components are standard and commercially available in the market.

2.4 Tire Properties

Loeb *et al*. examined on the relaxation length of a tire in [14]. The mechanical characteristics of the pneumatic tire have a large influence on the vehicle handling performance and directional response. "Kinematic properties are those that occur when the tire is rolling on a surface. The mechanical properties consist of spring-like properties measured with the tire in a stationary condition [14]". The spring rate of the

tire is tested using a Firestone mechanical spring rate test rig. An increasing load is applied to the tire and the resulting deflections are recorded and then plotted. The lateral stiffness is determined by calculating the initial slope of this plot. Performing a least-squares curve fit on the measured data and evaluating the derivative of the resultant equation at zero deflection can find the slope. They concluded that the cornering stiffness and lateral stiffness of a tire might be used to estimate the relaxation length.

Chiesa and Rinonapli looked at a new mathematical model developed to account for nonlinearities between vehicles and tires in [15]. Lateral and vertical stiffness have basic influences on the behavior of the car in sudden and severe maneuvers; therefore, these two properties of the tire were investigated. They examined the behavior of the car in various types of maneuvers at a constant speed. The vertical flexibility of the tires is not constant and tends to reduce with the lateral force between the tire and the road. They increased the number of DOF of the model to include the roll of the unsuspended masses and the consequent increase in body roll in order to take account in a rigorous manner of this flexibility. The increase in DOF occurs because the roll is not opposed by the rigidity of the suspension alone but by a lower rigidity. The lower rigidity is due to the effect of the flexibility of the tires being in series with that of the suspensions. The mathematical model is a system of seven differential equations. Three of the equations involve lateral, yaw, and roll movements of the car and the other four of the equations involve the relative movements between the tread of the tires and the wheel due to lateral flexibility of the tires. An increase in the lateral reaction for equivalent values of tire slip angle and vertical load generally produces considerable improvements on the behavior of the vehicle. The negative side to this is that the frequency of oscillations to which the

vehicle is subjected in the final part of each test is in fact noticeably increased. A positive effect was the increase in the lateral elastic rigidity because it produced effects of more modest dimensions. Clearly, the lateral elastic rigidity was seen to be a factor that damps the oscillations of the vehicle. The task of the driver in holding the car on its path is increased if the oscillation of the car were numerous. By balancing the increase in the cornering stiffness with a simultaneous increase in the lateral elastic stiffness the designer has the possibility of eliminating or reducing this trouble. "The calculating procedure and the mathematical model adopted assist in general to forecasting the effects of any modification on the parameters of the car or of the tires without actually building the vehicle [15]". They concluded the evaluation of handling characteristics of a vehicle must consider the total dynamic system of the vehicle, which is, the sprung and unsprung masses, the suspension system, and the tires.

Taylor *et al*. investigated the vertical stiffness measured for a radial ply agricultural drive tire using five methods: Load-deflection, non-rolling vertical free vibration, non-rolling equilibrium load-deflection, rolling vertical free vibration, and rolling equilibrium load-deflection in [16]. At all inflation pressures, non-rolling free vibration resulted in the highest stiffness, and load-deflection and non-rolling equilibrium load deflection results were similar. "The natural frequency was measured by timing the small oscillations of each frame while they were suspended from the pivot point. Oscillations were initiated by pushing the frame, which was then allowed to move freely [16]". The range of motion for the tire increased when the vertical load on the tire was increased. The natural frequency, the mass moment of inertia of the frame assembly, and the distance from the pivot point of the frame to the axle were required to determine the

vertical stiffness for a given condition. The measurement method impacts the results because of the noticeable differences in vertical stiffness, leading the authors to believe the five methods caused bias in the results.

2.5 Vehicle Handling

Salaani *et al*. combined multi-body dynamics with subsystem models to provide state-of-the-art high fidelity vehicle handling dynamics for real-time simulation in [17]. The particular formulation chosen to represent the vehicle as closely as possible depends heavily on how the parameters are obtained from the physical system. The vehicle response effects to be modeled must be specified in the multi-body approach. The multi-body formalism in conjunction with other subsystems is needed to simulate a complete vehicle model. The multi-body recursive formulations can be used to model rigid-body nonlinear motions. They discovered that the vehicle subsystems have become the fundamentals to complement vehicle dynamics simulation. The vehicle subsystem models are as important as rigid body dynamics.

Nalecz and Bindemann focused on the development of four-wheel steering systems for passenger vehicles in order to enhance their handling properties in [18]. Previous research on this subject is usually based on analysis of the classic 2-DOF linear bicycle model; however, by using the 2-DOF bicycle model important effects such as suspension kinematics, lateral weight transfer and chassis roll are ignored. Therefore, a non-linear 3-DOF vehicle model was used to represent each suspension as a three dimensional mechanism. They also used spatial kinematics to simulate suspension motion, giving the simulation the ability to determine the change in wheel steer and camber angles caused by chassis roll. These two men neglected aerodynamics. By doing

this, the only forces and moments, which act on the vehicle, are gravity, and those produced by the tires at the four contact patches. "The model is a 3-DOF, three mass model that consists of a sprung mass and the unsprung masses of front and rear suspension systems, which are connected to the sprung mass through the vehicle roll axis. The 3-DOF used for the vehicle model is lateral displacement, vehicle yaw and the sprung mass roll angle [18]". They determined that suspension kinematics, bump and roll steer influence vehicle response. The results showed that suspension and steering systems should be designed to either minimize the effects of bump and roll steer, or use these effects to enhance vehicle stability and response.

Mousseau *et al*. focused on the advent of multi-body system simulations (MSS) programs in [19]. MSS was effective in predicting the handling performance of vehicles; but not as successful in predicting the vehicle response at frequencies that are of interest in ride harshness and durability applications. For instance, when traveling on flat surfaces a rigid body vehicle model may prove adequate for predicting the handling response. On the other hand, a rigid body vehicle may prove inadequate for simulating a vehicle traveling over irregular terrain, since high-frequency modes may be excited in the vehicle and tire structure. They simulated the vehicle with a MSS program. The tires were simulated with nonlinear FE programs. A simple 2-DOF-vehicle dynamics model and a single-tire FE model were used for this approach. They assume that rigid bodies can adequately represent components with significant masses. "The results of this study indicate that this approach is a viable technique for simulating vehicle dynamic response on rough roads [19]".

CHAPTER 3: VIBRATION, PARAMETRIC AND SENSITIVITY ANALYSIS

3.1 Introduction

This chapter deals with the theoretical analysis for free and forced vibration. The results will also include cases for parametric and sensitivity analysis. The purpose of the theoretical analysis using realistic values is to show what happens under real conditions.

3.2 Vibration Analysis

3.2.1 Free Vibration

Systems that require two independent coordinates to describe their motion are called two DOF systems. Consider the system shown in Figure 3.1, in which a mass m is supported on two springs. Assuming that the mass is constrained to move in a vertical plane, the position of the mass, m, at any time can be specified by a linear coordinate $u(t)$, indicating the vertical displacement of the center of gravity of the mass, and an angular coordinate $\theta(t)$, denoting the rotation of the mass m about its center of gravity. Thus, the system has two degrees of freedom. It is important to note that in this case the mass m is not treated as a point mass, but as a rigid body having two possible types of motion. There are two equations of motion for a two DOF system and are generally in the form of coupled differential equations; that is, each equation involves all the coordinates.

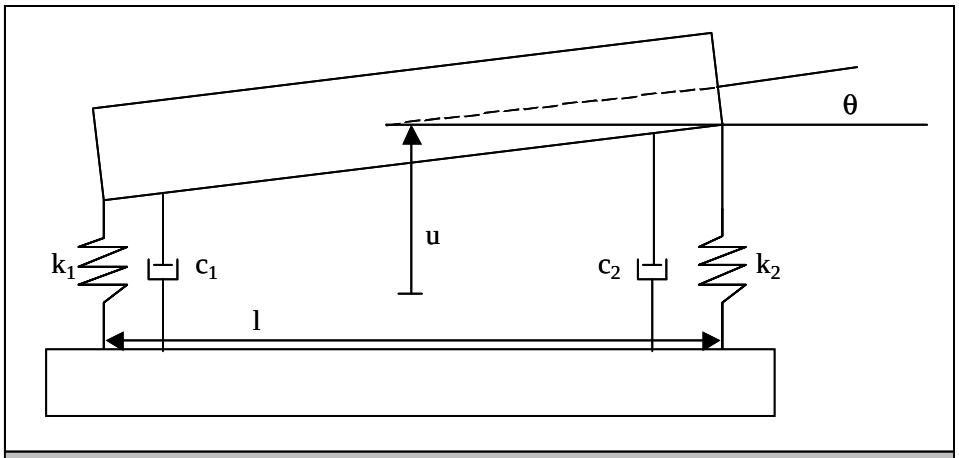

Figure 3.1: 2-degree of freedom system

From the Free Body Diagram in Figure 3.1, the equations of motion can be obtained. With the positive values of the motion variables as indicated, the force equilibrium equation in the vertical direction can be written as

$$\sum F_u = ma_u$$

$$m\ddot{u} = -k_1\left(u - \frac{l}{2}\theta\right) - k_2\left(u + \frac{l}{2}\theta\right) - c_1\left(\dot{u} - \frac{l}{2}\dot{\theta}\right) - c_2\left(\dot{u} + \frac{l}{2}\dot{\theta}\right) \tag{3.1}$$

or equivalently,

$$m\ddot{u} + (c_1 + c_2)\dot{u} - \frac{l}{2}(c_1 - c_2)\dot{\theta} + (k_1 + k_2)u - \frac{l}{2}(k_1 - k_2)\theta = 0. \tag{3.2}$$

The moment equation about the C.G. can be expressed as

$$\sum M_G = I_G\alpha$$

$$I_G\ddot{\theta} = \frac{k_1 l}{2}\left(u - \frac{l}{2}\theta\right) - \frac{k_2 l}{2}\left(u + \frac{l}{2}\theta\right) + \frac{c_1 l}{2}\left(\dot{u} - \frac{l}{2}\dot{\theta}\right) - \frac{c_2 l}{2}\left(\dot{u} + \frac{l}{2}\dot{\theta}\right) = 0 \tag{3.3}$$

or equivalently,

$$I_G\ddot{\theta} - \frac{l}{2}(c_1 - c_2)\dot{u} + \frac{l^2}{4}(c_1 + c_2)\dot{\theta} - \frac{l}{2}(k_1 - k_2)u + \frac{l^2}{4}(k_1 + k_2)\theta = 0. \tag{3.4}$$

Equations (3.2) and (3.4) can be rearranged and written in matrix form as

$$\begin{bmatrix} m & 0 \\ 0 & I_G \end{bmatrix}\begin{Bmatrix} \ddot{u} \\ \ddot{\theta} \end{Bmatrix} + \begin{bmatrix} c_1 + c_2 & -\frac{l}{2}(c_1 - c_2) \\ -\frac{l}{2}(c_1 - c_2) & \frac{l^2}{4}(c_1 + c_2) \end{bmatrix}\begin{Bmatrix} \dot{u} \\ \dot{\theta} \end{Bmatrix} + \begin{bmatrix} (k + k_2) & -\frac{l}{2}(k_1 - k_2) \\ -\frac{l}{2}(k_1 - k_2) & \frac{l^2}{4}(k_1 + k_2) \end{bmatrix}\begin{Bmatrix} u \\ \theta \end{Bmatrix} = \begin{Bmatrix} 0 \\ 0 \end{Bmatrix} \quad (3.5)$$

During free vibration at one of the natural frequencies, the amplitudes of the two DOF (coordinates) are related in a specific manner and the configuration is called a normal mode, principal mode, or natural mode of vibration. The system has damped natural frequencies instead of natural frequencies because there is damping in the system. The damped natural frequency is essentially, $\omega_d = \omega_n\sqrt{1-\zeta^2}$, where ζ is the damping ratio. Thus a two DOF system has two normal modes of vibration corresponding to the two damped natural frequencies.

Now the equations of motion can be used to obtain the poles (eigenvalues) and modes shapes (eigenvectors) for free vibration. A published article on tire parameters states that for a single tire, the tire spring and damping rates usually fall into the ranges of 175 to 300 kN/m and 0.35-0.70 kN-s/m, respectively [20]. The values for m, l_1, and l are taken from the 2002 Honda CR-V model. The values for k_1, k_2, c_1, and c_2 are picked arbitrarily from the published ranges given previously. Hence, the values for the parameters are the following:

$$m = 2519\,kg,\ l_1 = 2.53\,m,\ l = 2.95\,m,\ k_1 = 450\ kN/m,\ k_2 = 600\ kN/m,$$
$$c_1 = 1\ kN - `s/m,\ c_2 = 1.2\ kN - s/m$$

where m is the mass in kilograms, l_1 is the distance from the mass center to end of rigid body, l is the distance between front spring to rear spring, c_1 and k_1 are the spring and damping rate for both front tires, and c_2 and k_2 are the spring and damping rate for both rear tires. Note in the pages remaining, matrices are represented in bold capital letters and vectors are represented as bold lowercase letters.

For free vibration, the general equations of motion are of the form

$$\mathbf{M}\ddot{\mathbf{u}} + \mathbf{C}\dot{\mathbf{u}} + \mathbf{K}\mathbf{u} = \mathbf{0}\,. \tag{3.6}$$

A first order realization of Equation (3.6) is

$$\begin{bmatrix} \mathbf{0} & \mathbf{I} \\ -\mathbf{K} & \mathbf{0} \end{bmatrix}\begin{pmatrix} \mathbf{u} \\ \dot{\mathbf{u}} \end{pmatrix} - \begin{bmatrix} \mathbf{I} & \mathbf{0} \\ \mathbf{C} & \mathbf{M} \end{bmatrix}\begin{pmatrix} \dot{\mathbf{u}} \\ \ddot{\mathbf{u}} \end{pmatrix} = \begin{pmatrix} \mathbf{0} \\ \mathbf{0} \end{pmatrix} \tag{3.7}$$

where

$$\mathbf{A} = \begin{bmatrix} \mathbf{0} & \mathbf{I} \\ -\mathbf{K} & \mathbf{0} \end{bmatrix}, \tag{3.8}$$

$$\mathbf{B} = \begin{bmatrix} \mathbf{I} & \mathbf{0} \\ \mathbf{C} & \mathbf{M} \end{bmatrix} \tag{3.9}$$

and

$$\mathbf{z} = \begin{pmatrix} \mathbf{u} \\ \dot{\mathbf{u}} \end{pmatrix}. \tag{3.10}$$

This leads to

$$\mathbf{A}\mathbf{z} - \mathbf{B}\dot{\mathbf{z}} = \mathbf{0}\,. \tag{3.11}$$

The response of this system takes the form

$$\mathbf{z}(t) = \mathbf{v}e^{\lambda t} \tag{3.12}$$

where $\mathbf{v}$ is a constant vector. Substituting (3.12) in (3.11) leads to the eigenvalue problem

$$(\mathbf{A} - \lambda\mathbf{B})\mathbf{v} = \mathbf{0}. \tag{3.13}$$

In this context the vector $\mathbf{v}$ is called the eigenvector and λ are the eigenvalues. Further results are done using MATLAB. The simulation results are shown in Table 3.1 and Figures 3.2-3.6. The system is stable when the real part of all poles is negative as indicated in Figure 3.2. In Table 3.2, V1 and V2 are a complex conjugate pair and V3 and V4 are also a complex conjugate pair of vectors. With complex numbers in vibration, the real part is associated with the damping in the system and the imaginary part is associated with the frequency in the system.

Table 3.1: Poles of the system

Poles	Value
s_{11}	-0.43796 +20.51711i
s_{22}	-0.43796 -20.51711i
s_{33}	-0.14714 +11.71941i
s_{44}	-0.14714 -11.71941i

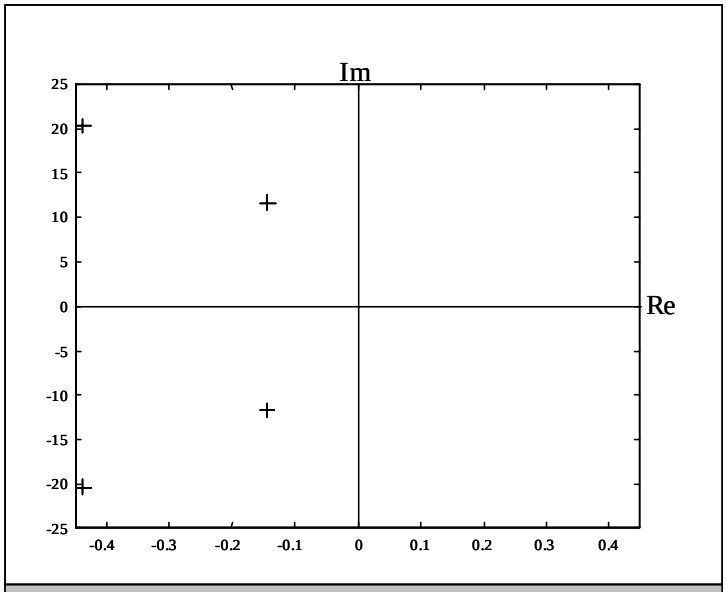

Figure 3.2: Poles of the system for free vibration

Table 3.2: Eigenvectors of the system			
V1	V2	V3	V4
0.0486 - 0.0004i	0.0486+0.0004i	-0.0031+0.0253i	-0.0031-0.0253i
0.0024 - 0.0001i	0.0024+0.0001i	0.0106-0.0804i	0.0106+0.0804i
-0.0124+0.9975i	-0.0124-0.9975i	-0.296-0.0401i	-0.296+0.0401i
0.0001 + 0.0490i	0.0001-0.0490i	0.9408+0.1357i	0.9408-0.1357i

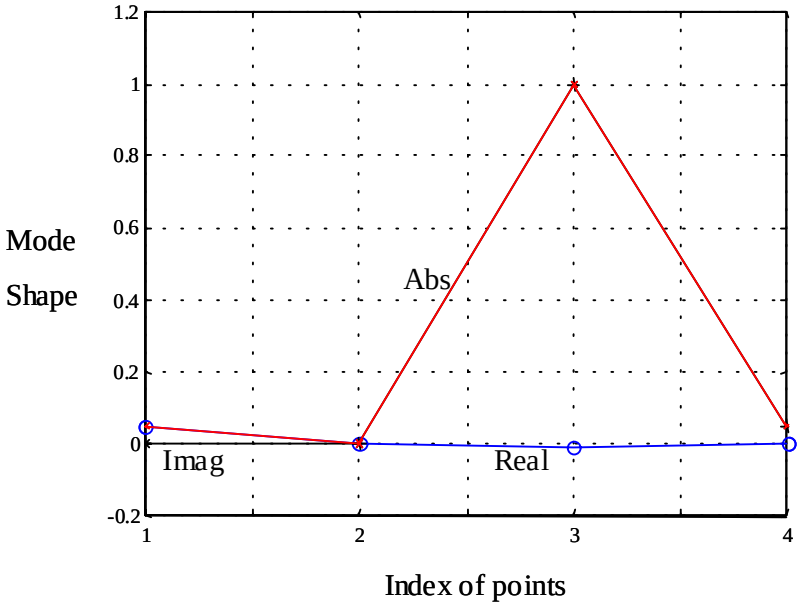

Figure 3.3: First mode shape (absolute, real and imaginary part)

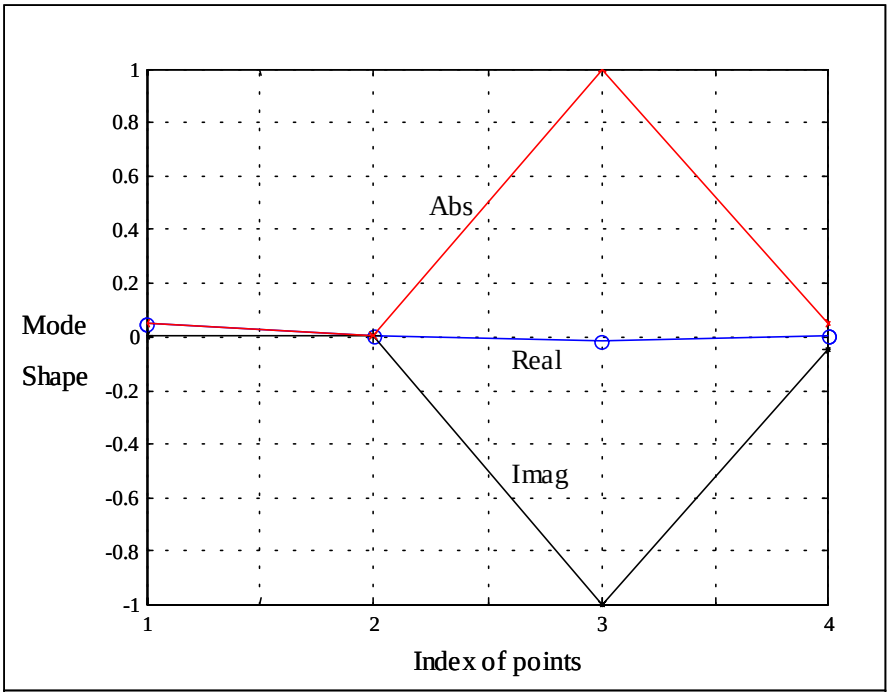

Figure 3.4: Second Mode (absolute, real and imaginary part)

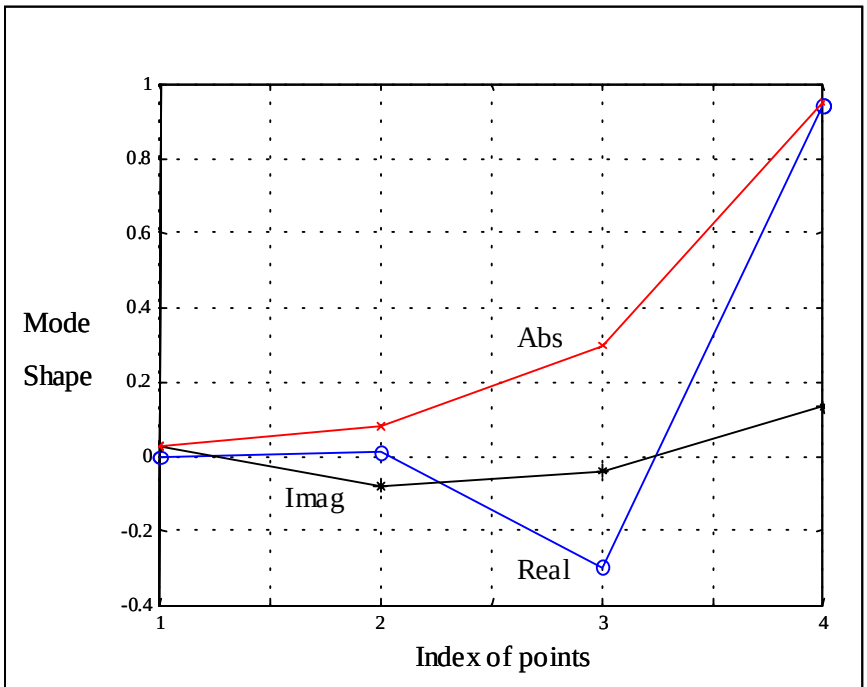

Figure 3.5: Third Mode (absolute, real and imaginary part)

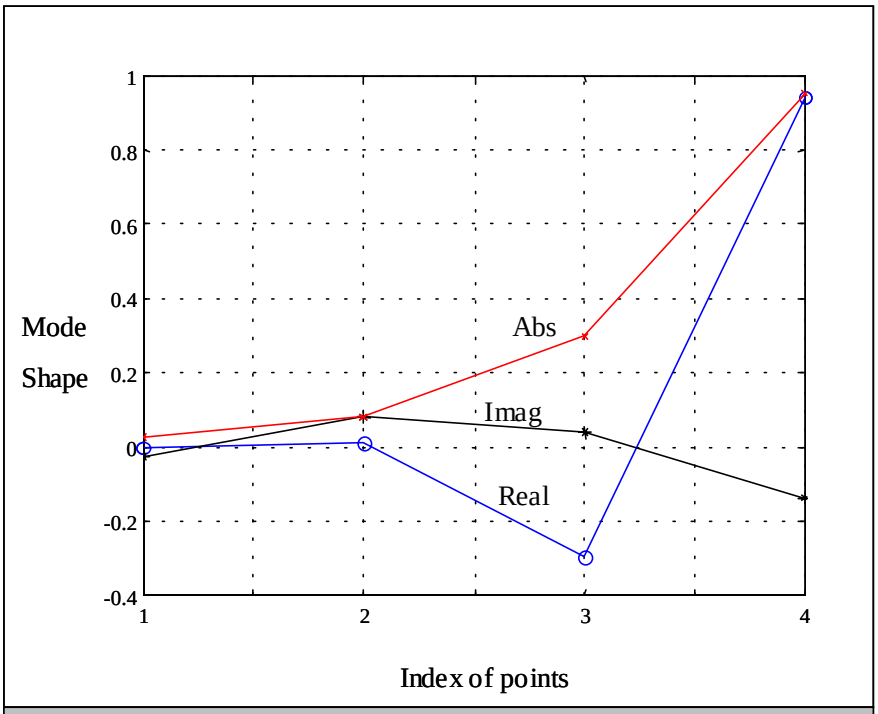

Figure 3.6: Fourth Mode (absolute, real and imaginary part)

3.2.2 Forced Vibration (Harmonic Excitation)

In general, the dynamic of a harmonically excited n degree-of-freedom system is governed by the equations

$$\mathbf{M}\ddot{\mathbf{u}} + \mathbf{C}\dot{\mathbf{u}} + \mathbf{K}\mathbf{u} = \mathbf{g}\sin\omega t + \mathbf{h}\cos\omega t \tag{3.14}$$

$$\mathbf{u}(0) = \mathbf{x}_0,\ \dot{\mathbf{u}}(0) = \mathbf{v}_0 \tag{3.15}$$

where $\mathbf{g}, \mathbf{h}, \mathbf{x}_0$ and $\mathbf{v}_0$ are constant vectors. The solution of the problem can be obtained by solving two simpler problems. The first associated with the homogeneous solution, the other with the particular solution, and then superimposing the results. This means,

$$\mathbf{u}(t) = \mathbf{u}_P(t) + \mathbf{u}_H(t) \tag{3.16}$$

where $\mathbf{u}_P$ is the particular solution of

$$\mathbf{M}\ddot{\mathbf{u}}_P + \mathbf{C}\dot{\mathbf{u}}_P + \mathbf{K}\mathbf{u}_P = \mathbf{g}\sin\omega t + \mathbf{h}\cos\omega t\,. \tag{3.17}$$

Trying a solution of the form

$$\mathbf{u}_p(t) = \mathbf{p}\cos\omega t + \mathbf{q}\sin\omega t \tag{3.18}$$

leads to the matrix

$$\begin{bmatrix} \mathbf{K}-\omega^2\mathbf{M} & \omega\mathbf{C} \\ -\omega\mathbf{C} & \mathbf{K}-\omega^2\mathbf{M} \end{bmatrix}\begin{pmatrix} \mathbf{p} \\ \mathbf{q} \end{pmatrix} = \begin{pmatrix} \mathbf{h} \\ \mathbf{g} \end{pmatrix} \tag{3.19}$$

which determines $\mathbf{p}$ and $\mathbf{q}$ giving the solution $\mathbf{u}_p(t)$.

The general solution, $\mathbf{u}_\mathbf{H}$, which depends on an arbitrary combination of $2n$ linearly independent functions, of the homogeneous problem

$$\mathbf{M}\ddot{\mathbf{u}}_\mathbf{H} + \mathbf{C}\dot{\mathbf{u}}_\mathbf{H} + \mathbf{K}\mathbf{u}_\mathbf{H} = 0. \tag{3.20}$$

Trying a solution of the form

$$\mathbf{u}_H = \mathbf{r}e^{st} \tag{3.21}$$

where s is the eigenvalues and $\mathbf{r}$ is the eigenvector. A more general solution of Equation (3.20) is

$$\mathbf{u}_H = \sum_{j=1}^{2n} a_j \mathbf{r}_j e^{s_j t} \tag{3.22}$$

and is expressed as a combination of $2n$ linearly independent functions where a_j are constants. The step-by-step formulation to obtain the eigenvalue problem for the homogenous solution is already given in Equations (3.6)-(3.13).

The homogeneous solution is what was covered in Section 3.2.1; therefore the particular solution is of more interest. The equations of motion for forced vibration for the system in Figure 3.7, where $\mathbf{h} = \mathbf{0}$, are as follows,

$$\begin{bmatrix} m & 0 \\ 0 & I_G \end{bmatrix}\begin{Bmatrix} \ddot{\mathbf{u}} \\ \ddot{\boldsymbol{\theta}} \end{Bmatrix}+\begin{bmatrix} c_1+c_2 & -\frac{l}{2}(c_1-c_2) \\ -\frac{l}{2}(c_1-c_2) & \frac{l^2}{4}(c_1+c_2) \end{bmatrix}\begin{Bmatrix} \dot{\mathbf{u}} \\ \dot{\boldsymbol{\theta}} \end{Bmatrix}$$
$$+\begin{bmatrix} (k+k_2) & -\frac{l}{2}(k_1-k_2) \\ -\frac{l}{2}(k_1-k_2) & \frac{l^2}{4}(k_1+k_2) \end{bmatrix}\begin{Bmatrix} \mathbf{u} \\ \boldsymbol{\theta} \end{Bmatrix}=\begin{Bmatrix} \mathbf{g}\sin\omega t \\ 0 \end{Bmatrix} \quad (3.23)$$

The solution for Equation (3.23) can also be written in the form

$$\mathbf{u}(t)=\mathbf{U}\sin(\omega t-\boldsymbol{\Theta}) \quad (3.24)$$

where $\mathbf{U}$ is the magnitude and $\boldsymbol{\Theta}$ is the phase function. Equation (3.23) is the governing equation and computer simulations will be used for further results. The results are shown in Figures 3.8 to 3.11.

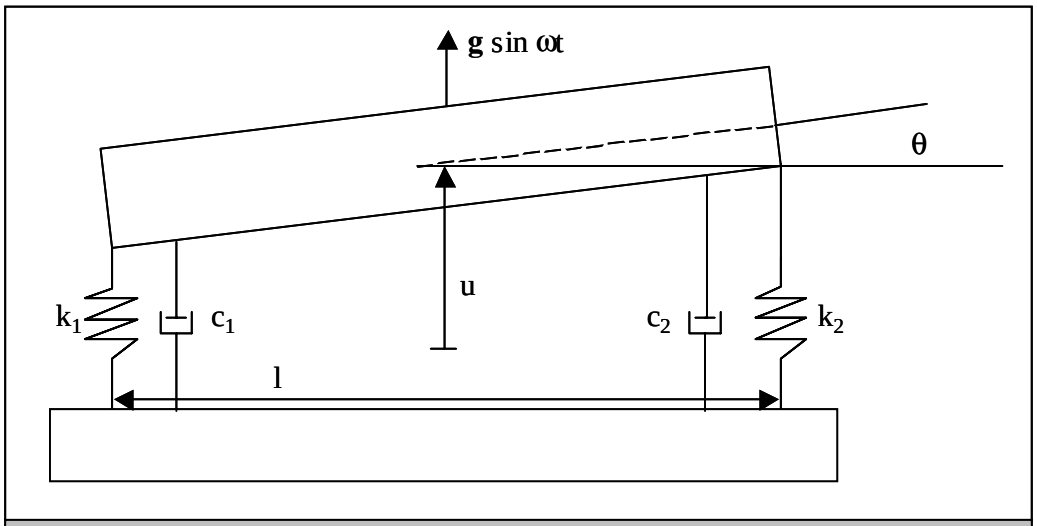

Figure 3.7: 2-degree of freedom system with external force

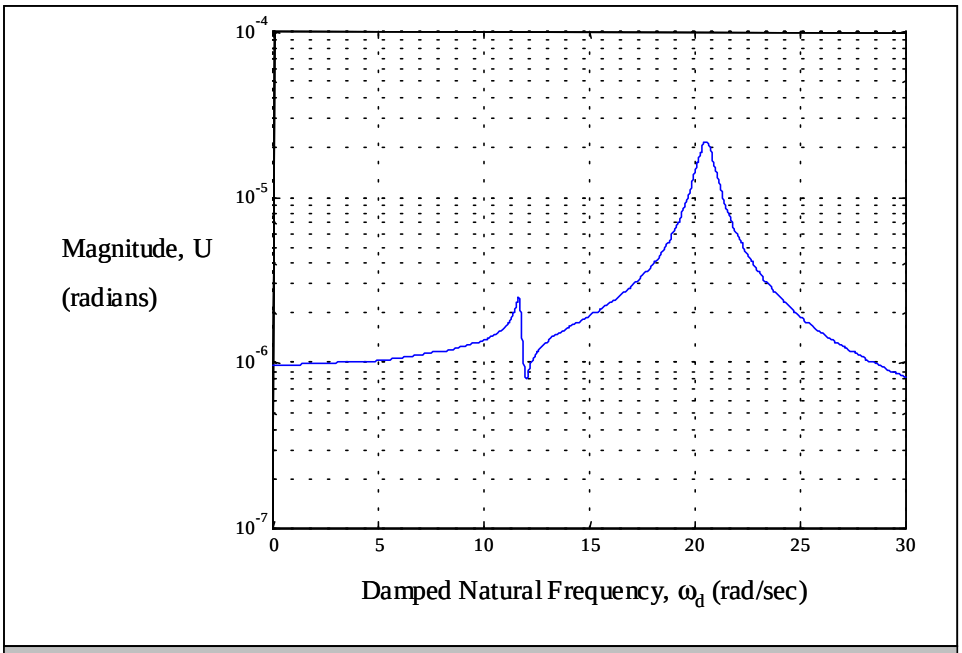

Figure 3.8: Magnitude in bounce mode for forced vibration

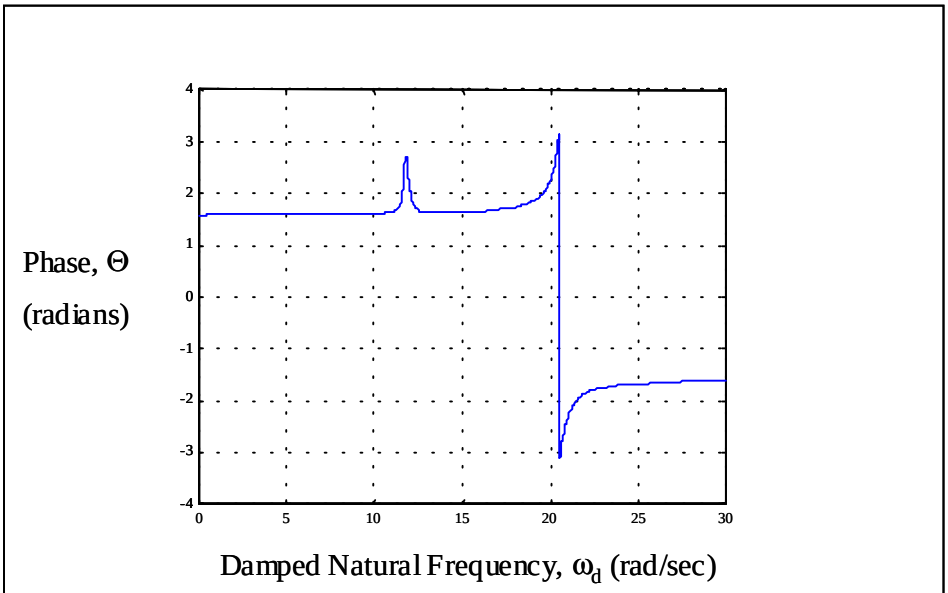

Figure 3.9: Phase function in bounce mode for forced vibration

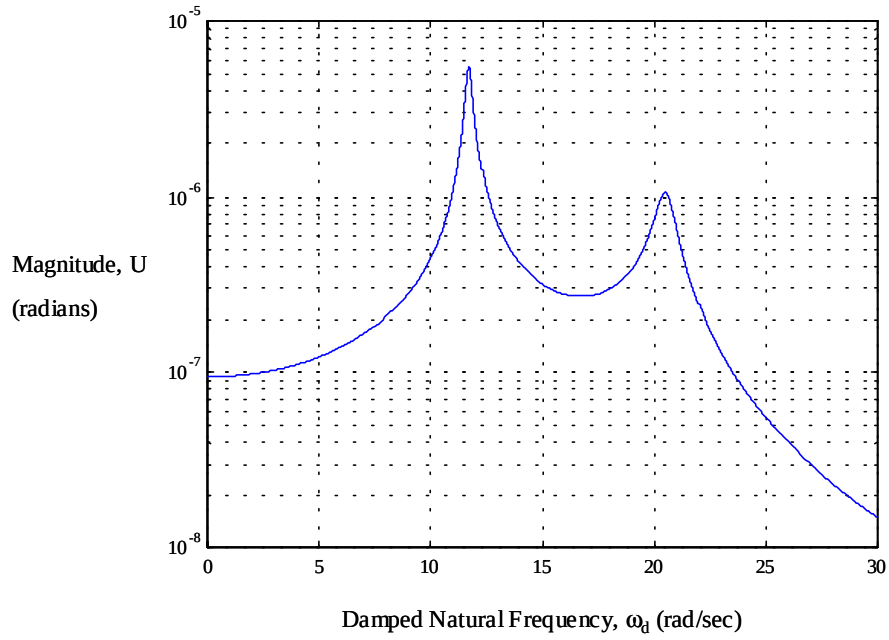

Figure 3.10: Magnitude in pitch mode for forced vibration

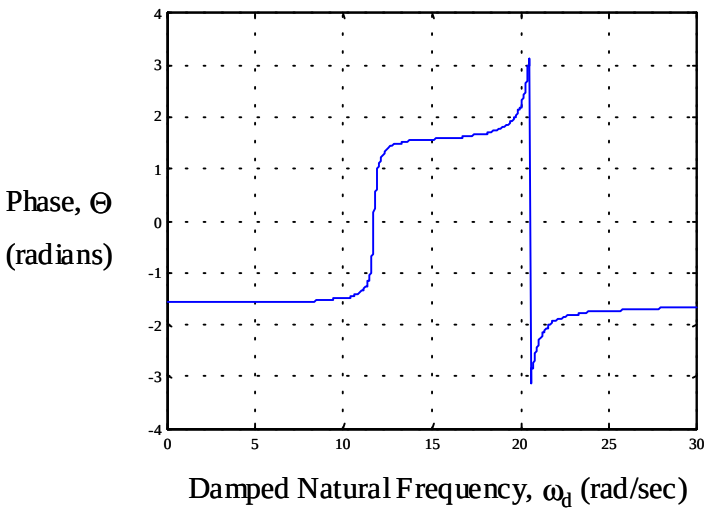

Figure 3.11: Phase function in pitch mode for forced vibration

By not specifying a specific value for the frequency of the external force allows for a parametric analysis to see when large amplitude of vibration occurs. Figure 3.8 to

3.11 show what happens when large amplitude of vibration occurs. Large amplitude vibration is when the frequency of the external force coincides with one of the damped natural frequencies of the system, and the system undergoes dangerously large oscillations.

3.3 Parametric Analysis

Parametric studies of dynamical systems are an important task in all major engineering design. This is especially true in the design of control systems, when the focus is for low sensitivity to parameter variations. It is important to know when one parameter is changed, how that affects the system; if the system becomes unstable, do the natural frequencies change, etc. These are things to consider when attempting building a system.

In the analyses below, all parameters are held constant except one. Table 3.3 shows the initial value, Δ_0, of each parameter as well as the new value after the i^{th} incremental change, Δ_i. The increments for each parameter are chosen arbitrarily at equal intervals. However, each parameter was not to exceed a certain limit. For example, m was not to exceed the maximum load carried by the vehicle, l_1 was not to exceed the total length of the vehicle, k_1 and c_1 were not to exceed published ranges for stiffness and damping of a vehicle. Hence, on each of the graphs following, there will be six curves to represent the initial value and five incremental changes to the parameter.

Table 3.3: Ranges for each parameter for parametric analysis						
	Δ_0	Δ_1	Δ_2	Δ_3	Δ_4	Δ_5
m (kg)	2519	2719	2919	3119	3319	3519
l_1 (m)	2.53	2.63	2.73	2.83	2.93	3.03
k_1 (kN/m)	450	454	458	462	466	470
c_1 (kN-s/m)	1000	1020	1040	1060	1080	1100

The first parametric analysis is on the mass moment of inertia, J. It is possible to change J without changing the mass by changing l_1. The simulation results are shown in Figures 3.12-3.15.

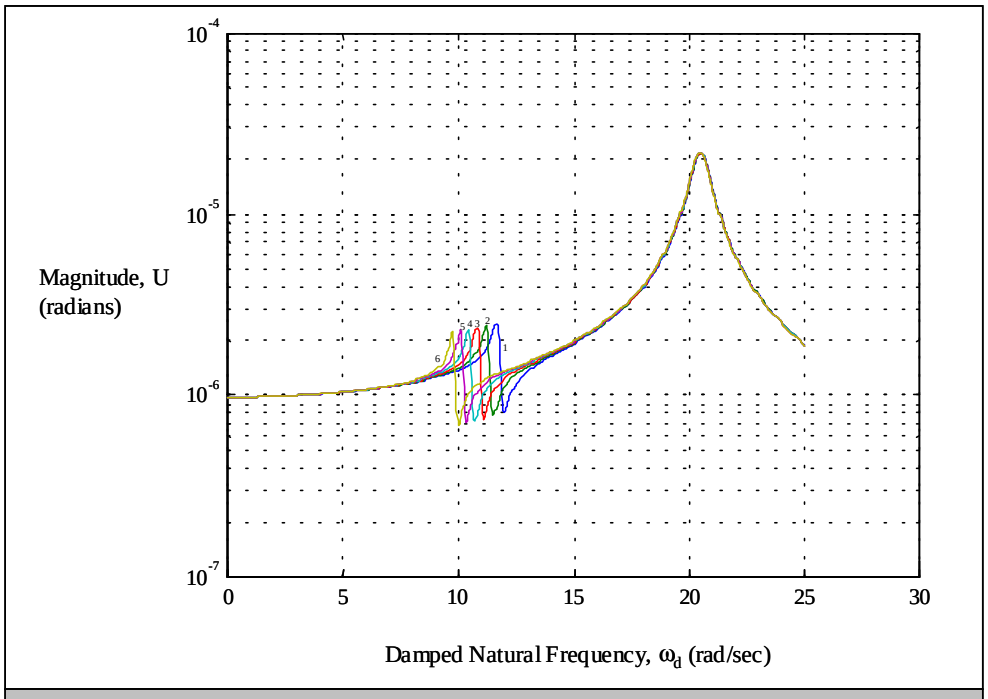

Figure 3.12: Parametric analysis for J-magnitude in bounce mode

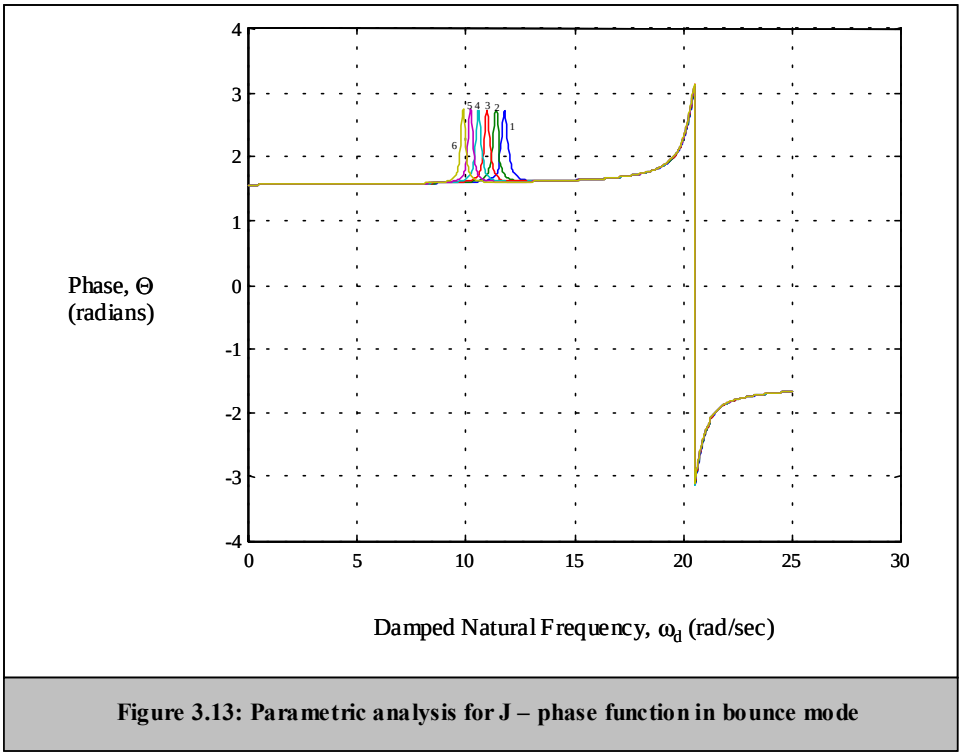

Figure 3.13: Parametric analysis for J – phase function in bounce mode

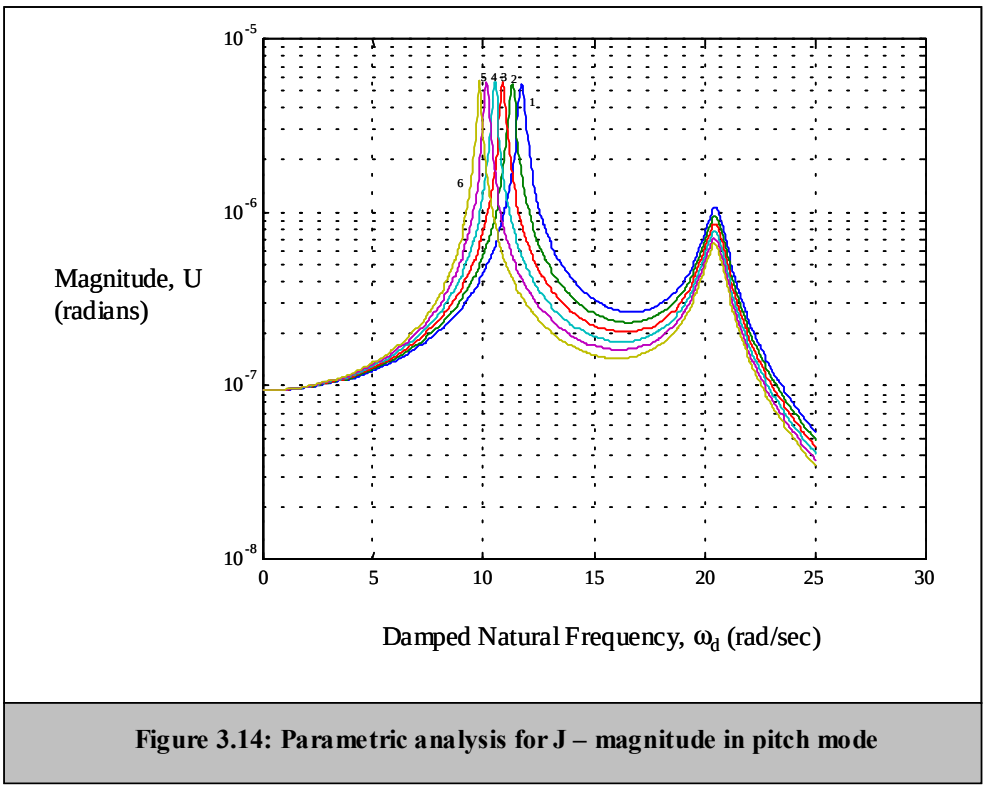

Figure 3.14: Parametric analysis for J – magnitude in pitch mode

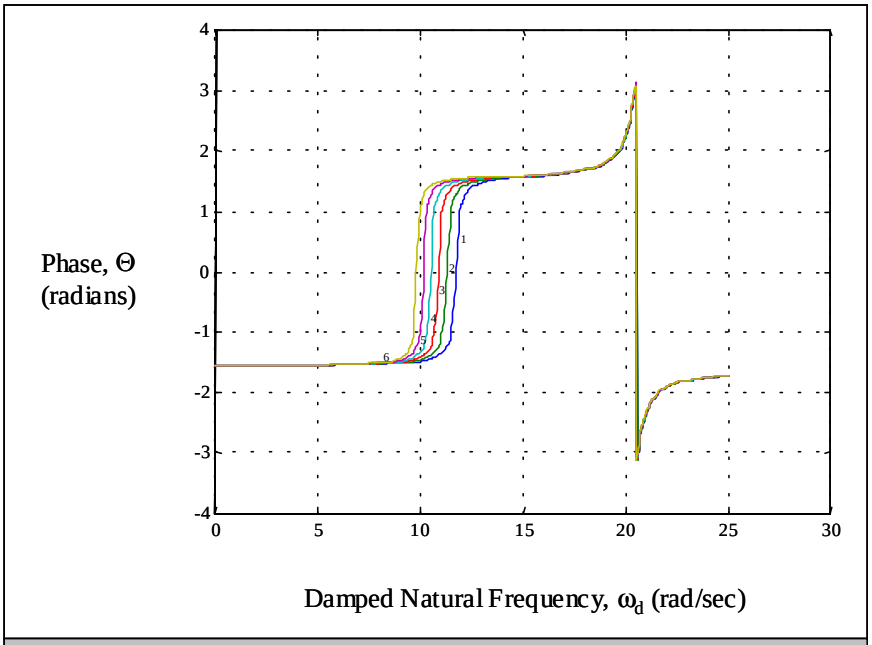

Figure 3.15: Parametric analysis for J – phase function in pitch mode

In Figures 3.12 and 3.14 it shows that when J is increased, the first damped natural frequency decreases from approximately 11.65 to 9.75 and decreases in magnitude slightly. The corresponding phase function for each increase is shown in Figures 3.13 and 3.15. For the first mode of vibration, as shown in Figures 3.12 and 3.13, J does not have any effect on the second damped natural frequency. In the pitch mode, the second damped natural frequency changes in magnitude only, whereas the first damped natural frequency decreases as shown in Figures 3.14 and 3.15.

The second parametric analysis is on the mass. Changing the mass also means the mass moment of inertia is affected as well. However, the effect that changing the mass will have on the system will still be seen. The simulation results are shown in Figures 3.16-3.19.

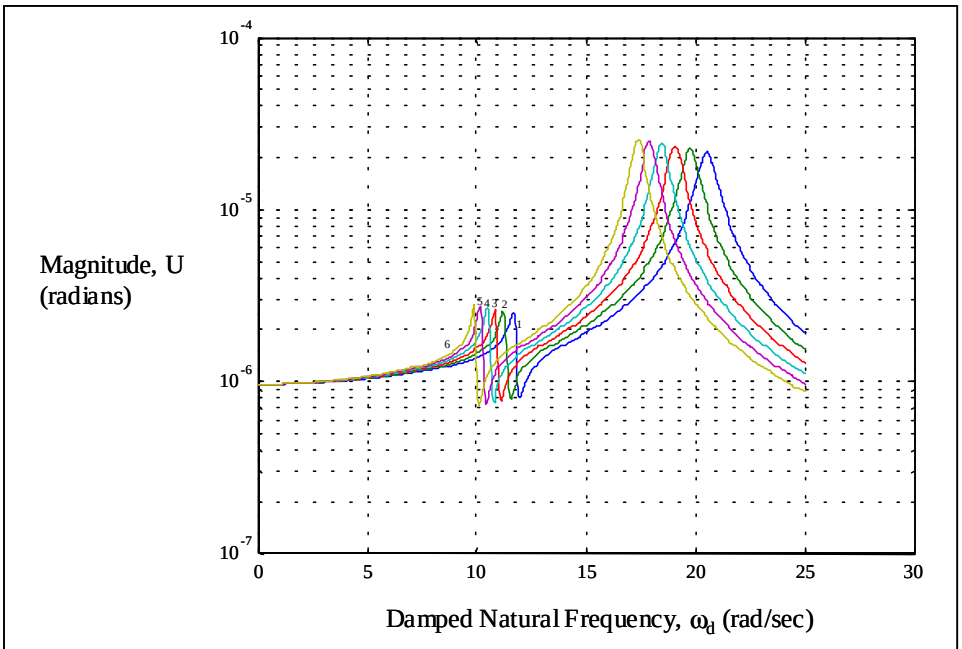

Figure 3.16: Parametric analysis for m – magnitude in bounce mode

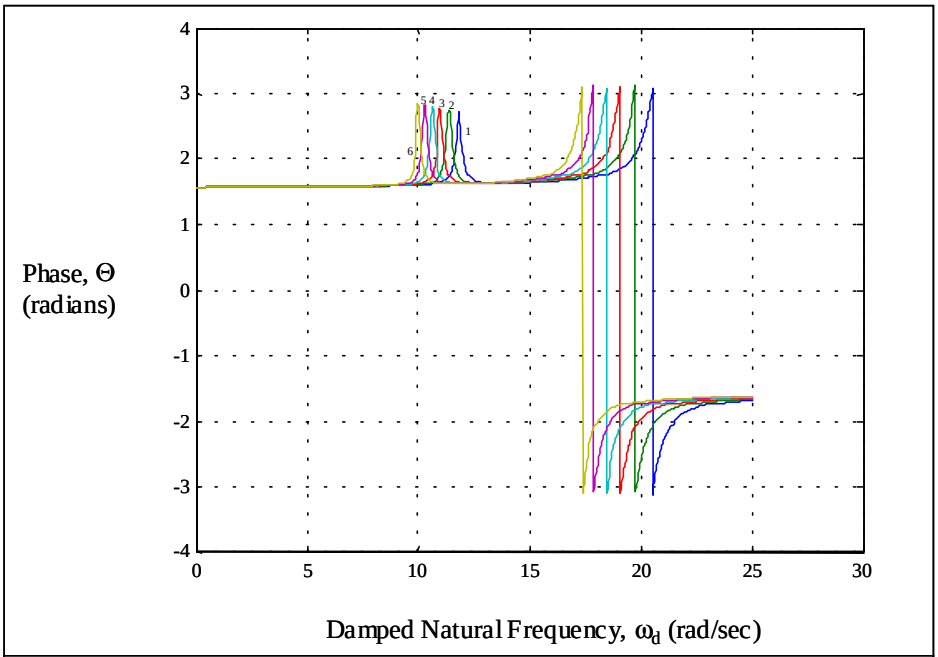

Figure 3.17: Parametric analysis for m – phase function in bounce mode

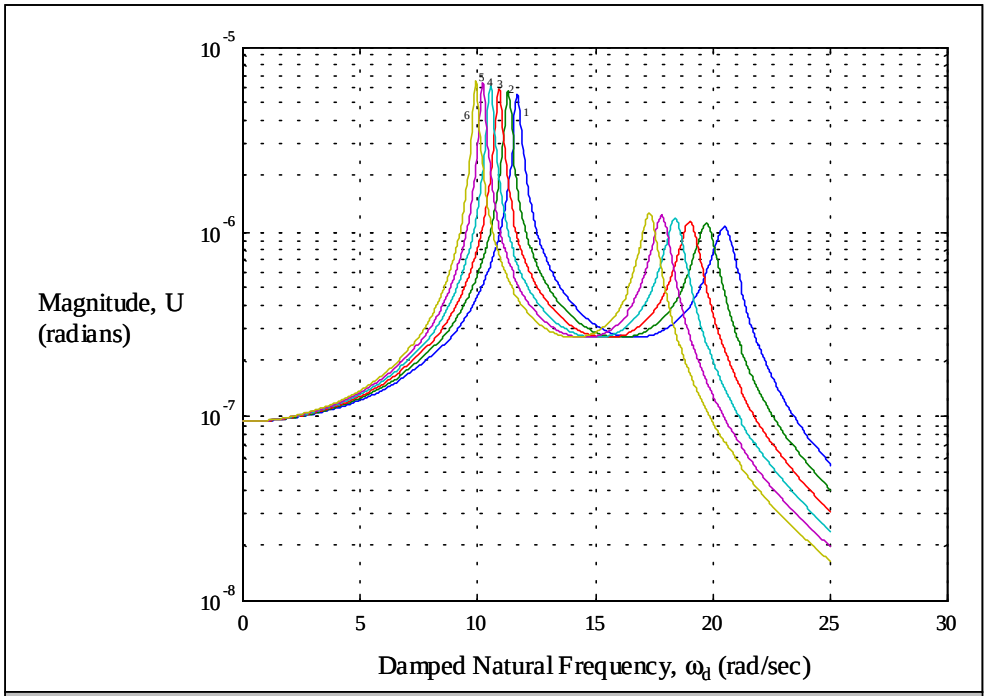

Figure 3.18: Parametric analysis for m – magnitude in pitch mode

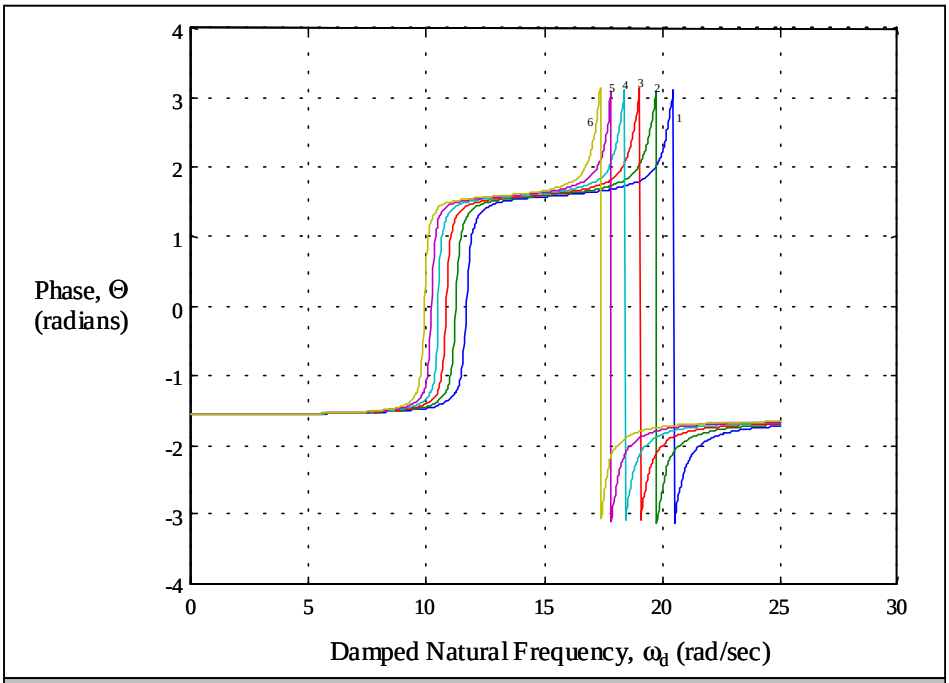

Figure 3.19: Parametric analysis for m – phase function in pitch mode

When the mass is changed, both damped natural frequencies decrease but their magnitude increases. Figures 3.16-3.19 show these changes. The damped natural frequency depends on the natural frequency; therefore, it follows from the parametric analysis that the damped natural frequency decreases as the mass increases. This is what should happen since $\omega_n = \sqrt{k/m}$.

The third parametric analysis is on the stiffness for the front tires, k_1. The simulation results are shown in Figures 3.20-3.23.

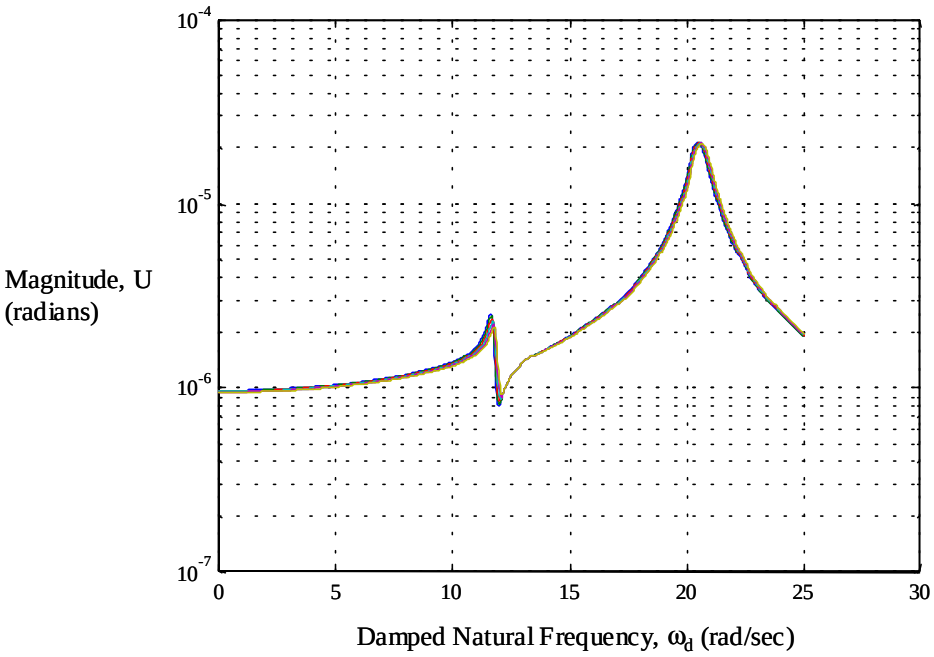

Figure 3.20: Parametric analysis for k_1 – magnitude in bounce mode

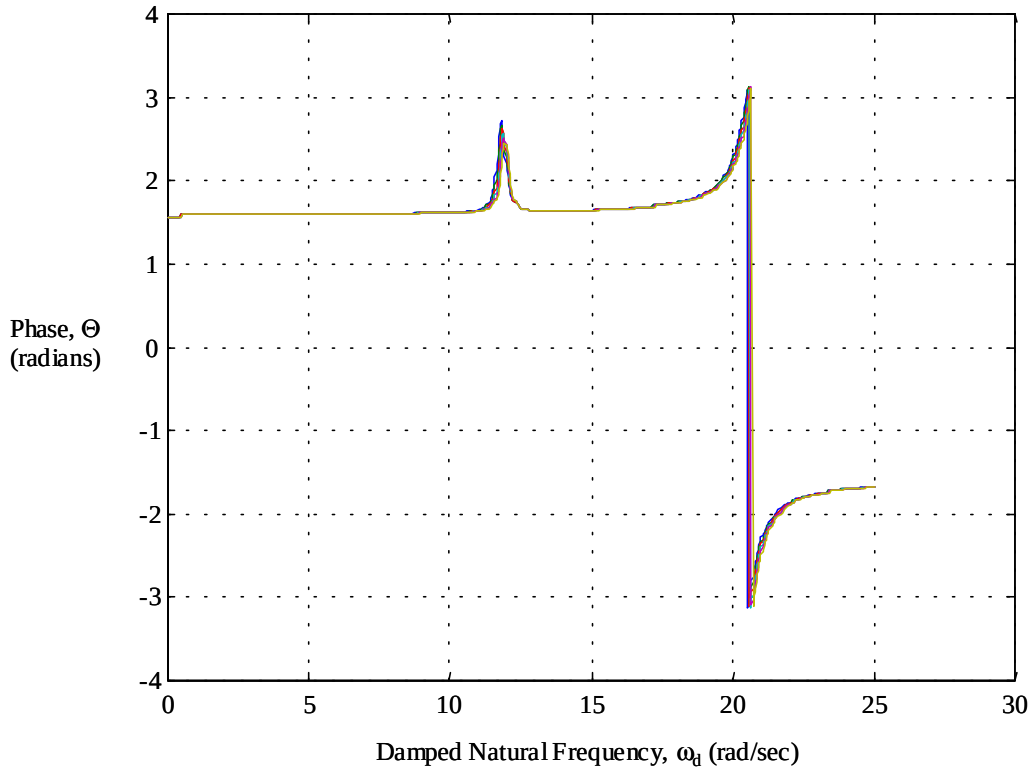

Figure 3.21: Parametric analysis for k_1 – phase function in bounce mode

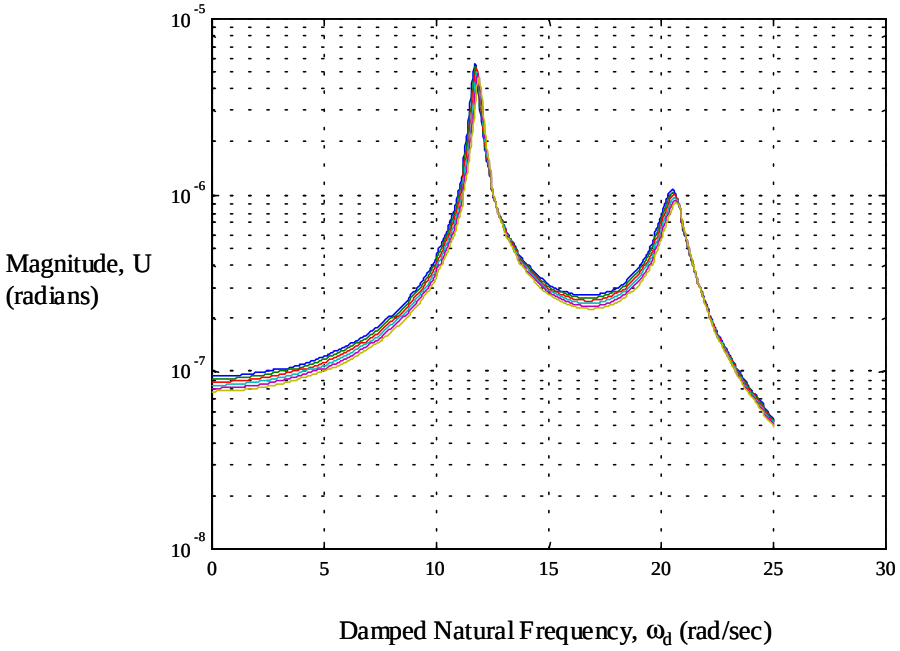

Figure 3.22: Parametric analysis for k_1 – magnitude in pitch mode

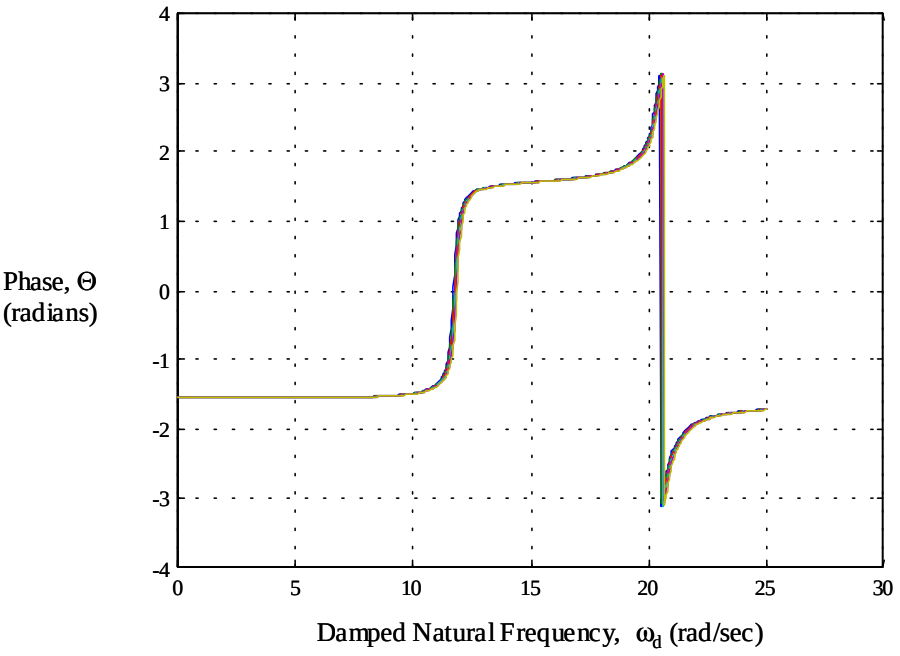

Figure 3.23: Parametric analysis for k_1 – phase function in pitch mode

There is a small effect of increasing k_1. Figure 3.20 shows the first damped natural frequency decreases very slightly, almost not noticeable by the human eye. Figures 3.21-3.23 show that both damped natural frequencies change positions slightly. The increase in the damped natural frequencies is what should happen, but the effect could be small because k_1 was increased by a small amount, trying not to exceed k_2 at the same time. This small effect is noticed in Figures 3.20-3.23 because at some points all the curves coincide. Although k_1 is only shown, the same thing happens when a parametric analysis is performed on k_2.

The fourth parametric analysis is on the damping for the front tires, c_1. The simulation results are shown in Figures 3.24-3.27.

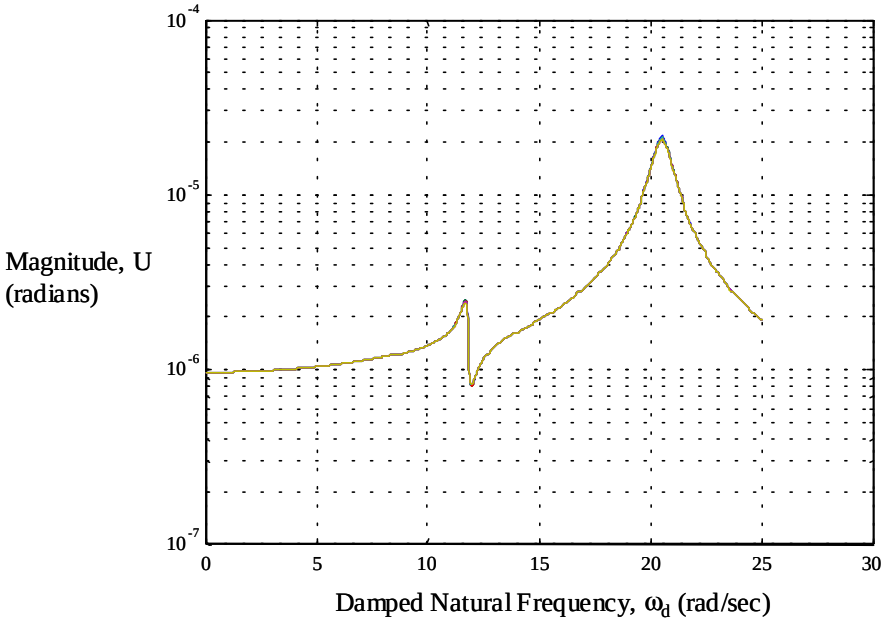

Figure 3.24: Parametric analysis for c_1 – magnitude in bounce mode

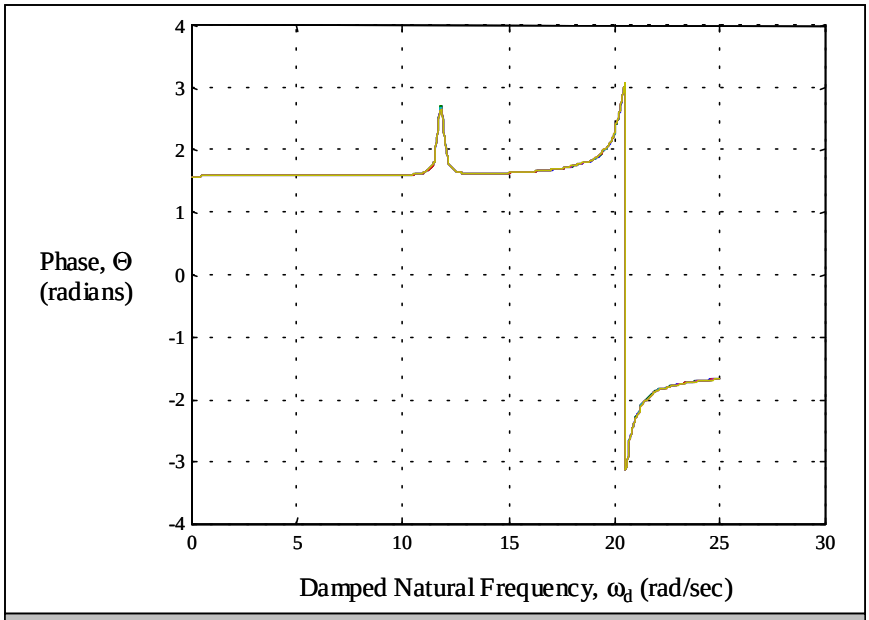

Figure 3.25: Parametric analysis for c_1 – phase function in bounce mode

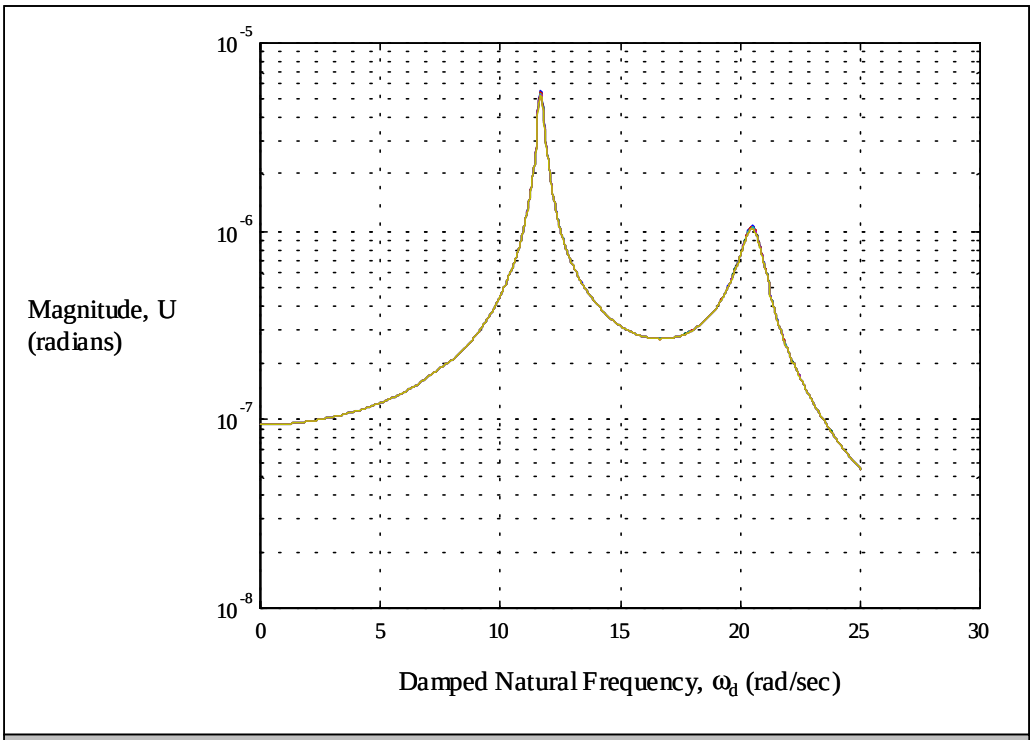

Figure 3.26: Parametric analysis for c_1 – magnitude in pitch mode

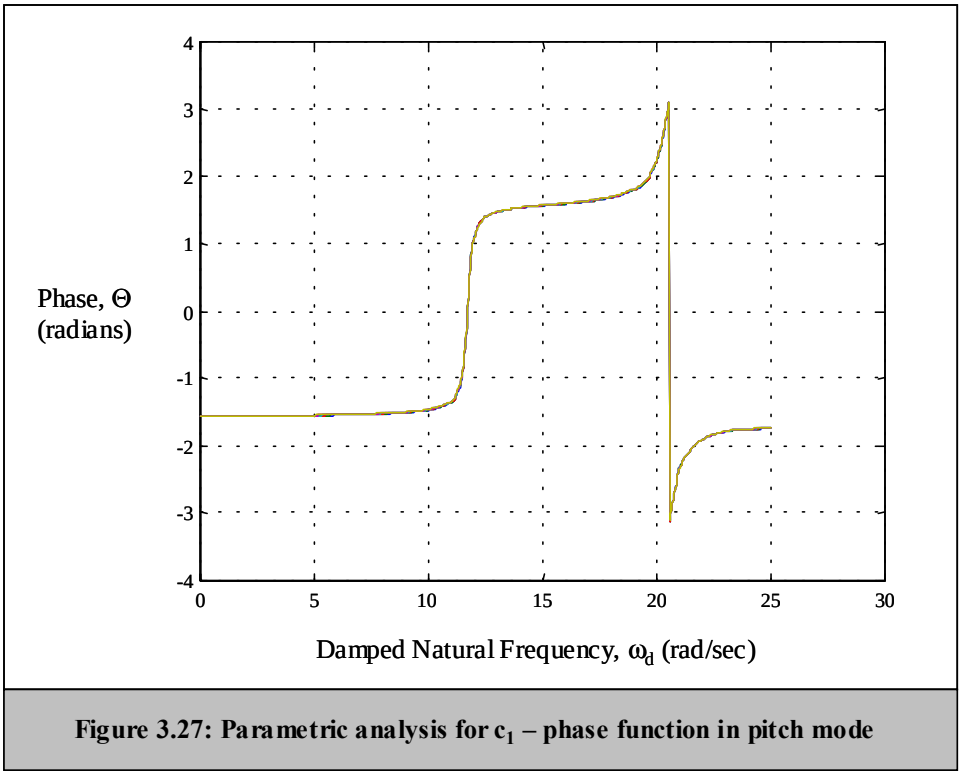

Figure 3.27: Parametric analysis for c_1 – phase function in pitch mode

Figures 3.24-3.27 show that the damping has no effect on the damped natural frequency. This indicates that ζ, the damping ratio, is very small such that $\omega_d \cong \omega_n$. Although c_1 is only shown, the same follows for c_2.

3.4 Sensitivity Analysis

3.4.1 Equations of Sensitivity

When performing a parametric analysis, it is necessary to consider the sensitivity of the system to perturbations. This study involves the problem of determining how sensitive is a parameter to a change in one or several other parameters. In general, it is important when designing a system to not have parameters, which are extremely sensitive to changes in the operating conditions. In dealing with vibration, the main concern is with the sensitivity of the natural frequencies, or the eigenvalues of the system.

Consider a linear time invariant system is governed by the set of differential equations

$$\dot{\mathbf{z}} = \mathbf{A}\mathbf{z}\,, \tag{3.25}$$

where $\mathbf{A} \in \Re^{2n\times 2n}$, and $\mathbf{z} \in \Re^{2n}$. The response of this system takes the form

$$\mathbf{z}(t) = \mathbf{x}e^{\lambda t}\,, \tag{3.26}$$

where $\mathbf{x}$ is a constant vector. Substituting (3.26) in (3.25) leads to the eigenvalue problem

$$(\mathbf{A} - \lambda\mathbf{I})\mathbf{x} = \mathbf{o}\,. \tag{3.27}$$

In this context the vector $\mathbf{x}$ is called a right eigenvector of $\mathbf{A}$. Generally, there are $2n$ eigenvalues λ_i, and $2n$ right eigenvectors $\mathbf{x}_i$, $i = 1,2,...,2n$. When $\mathbf{A}$ is not symmetric, it is useful to investigate the auxiliary eigenvalue problem associated with $\mathbf{A}^T$, namely

$$(\mathbf{A}^T - \lambda\mathbf{I})\mathbf{y} = \mathbf{o}\,. \tag{3.28}$$

The vector $\mathbf{y}$ is called a left eigenvector of $\mathbf{A}$. In general, there are $2n$ eigenvalues λ_i to the problem in Equation (3.28), which are the same as that of the problem in Equation (3.27), and $2n$ left eigenvectors $\mathbf{y}_i$, $i = 1,2,...,2n$. Obviously, if $\mathbf{A}$ is symmetric then $\mathbf{x}_i = \mathbf{y}_i$, since in this case the eigenvalue problems in Equation (3.27) and (3.28) are identical.

In many occasions, the matrix $\mathbf{A}$ is a function of a parameter, or several parameters a_i, i.e.

$$\mathbf{A} = \mathbf{A}(a_i, i = 1,2,..., p)\,.$$

The sensitivity of the eigenvalue λ_i to incremental change in the parameter a_k is given in [21]

$$\frac{\partial \lambda_i}{\partial a_k} = \frac{\mathbf{y}_i^T \dfrac{\partial \mathbf{A}}{\partial a_k} \mathbf{x}_i}{\mathbf{y}_i^T \mathbf{x}_i} \qquad i = 1,2,...,2n\,,\ k = 1,2,...,p \tag{3.29}$$

where $\dfrac{\partial \mathbf{A}}{\partial a_k}$ is the partial derivative of $\mathbf{A}$ with respect to a_k.

The right and left eigenvectors can be assembled in modal matrices as follows:

$$\mathbf{X} = \begin{bmatrix} \mathbf{x}_1 & \mathbf{x}_2 & \cdots & \mathbf{x}_{2n} \end{bmatrix},$$

and

$$\mathbf{Y} = \begin{bmatrix} \mathbf{y}_1 & \mathbf{y}_2 & \cdots & \mathbf{y}_{2n} \end{bmatrix}.$$

Then the relation between $\mathbf{X}$ and $\mathbf{Y}$ is

$$\mathbf{Y} = \left(\mathbf{X}^T\right)^{-1}. \tag{3.30}$$

Example

Let $\mathbf{A}$ be a 3×3 matrix depending on two parameters, a_1 and a_2,

$$\mathbf{A} = \begin{bmatrix} 3a_1 & -2 & -1 \\ 5 & 7a_2 & 3a_2 \\ 7 & 3 & 4a_1 \end{bmatrix}.$$

Differentiation with respect to a_1 and a_2 yields:

$$\frac{\partial \mathbf{A}}{\partial a_1} = \begin{bmatrix} 3 & 0 & 0 \\ 0 & 0 & 0 \\ 0 & 0 & 4 \end{bmatrix}$$

and

$$\frac{\partial \mathbf{A}}{\partial a_2} = \begin{bmatrix} 0 & 0 & 0 \\ 0 & 7 & 3 \\ 0 & 0 & 0 \end{bmatrix}.$$

The right and left eigenvectors of $\mathbf{A} - \lambda \mathbf{I}$ are:

$$\mathbf{X} = \begin{bmatrix} 0.1415 & -0.1109 & 0.0728 \\ 0.4520 & 0.5140 & -0.9928 \\ -0.8807 & -0.8506 & -0.0947 \end{bmatrix},$$

and

$$\mathbf{Y} = \begin{bmatrix} 4.0026 & -4.1104 & -0.3060 \\ 0.3247 & -0.2274 & -0.9771 \\ -0.3258 & -0.7770 & -0.5506 \end{bmatrix}.$$

In the neighborhood of $a_1 = 2.5$ and $a_2 = 5$, the sensitivity functions for the eigenvalues are

$$\frac{\partial \lambda_1}{\partial a_1} = \frac{\begin{pmatrix} 4.0026 & 0.3247 & -0.3258 \end{pmatrix} \begin{bmatrix} 3 & 0 & 0 \\ 0 & 0 & 0 \\ 0 & 0 & 4 \end{bmatrix} \begin{pmatrix} 0.1415 \\ 0.4520 \\ -0.8807 \end{pmatrix}}{\begin{pmatrix} 4.0026 & 0.3247 & -0.3258 \end{pmatrix} \begin{pmatrix} 0.1415 \\ 0.4520 \\ -0.8807 \end{pmatrix}} = 2.8466$$

$$\frac{\partial \lambda_1}{\partial a_2} = 0.1694$$

$$\frac{\partial \lambda_2}{\partial a_1} = 4.0116$$

$$\frac{\partial \lambda_2}{\partial a_2} = -0.2380$$

$$\frac{\partial \lambda_3}{\partial a_1} = 0.1417$$

$$\frac{\partial \lambda_3}{\partial a_2} = 7.0686 .$$

In order to confirm the results, the parameters were slightly perturbed and the associated change in the eigenvalues was inspected. For $a_1 = 2.5 + \Delta a_1$, where $\Delta a_1 = 0.001$, $\Delta \lambda_1 = 0.002847$. Hence, $\frac{\Delta \lambda_1}{\Delta a_1} = \frac{0.002847}{0.001} = 2.847$, which is a good approximation to the exact sensitivity obtained from Equation (3.29).

3.4.2 Sensitivity of vibrations

In vibration the equations of motion are usually expressed in a second order form

$$\mathbf{M}\ddot{\mathbf{u}} + \mathbf{C}\dot{\mathbf{u}} + \mathbf{K}\mathbf{u} = \mathbf{o} . \tag{3.31}$$

A first order realization of (3.31) is

$$\begin{bmatrix} \mathbf{I} & \mathbf{0} \\ \mathbf{0} & \mathbf{M} \end{bmatrix} \begin{pmatrix} \dot{\mathbf{u}} \\ \ddot{\mathbf{u}} \end{pmatrix} = \begin{bmatrix} \mathbf{0} & \mathbf{I} \\ -\mathbf{K} & -\mathbf{C} \end{bmatrix} \begin{pmatrix} \mathbf{u} \\ \dot{\mathbf{u}} \end{pmatrix} \tag{3.32}$$

so that

$$\begin{pmatrix} \dot{\mathbf{u}} \\ \ddot{\mathbf{u}} \end{pmatrix} = \begin{bmatrix} \mathbf{I} & \mathbf{0} \\ \mathbf{0} & \mathbf{M}^{-1} \end{bmatrix} \begin{bmatrix} \mathbf{0} & \mathbf{I} \\ -\mathbf{K} & -\mathbf{C} \end{bmatrix} \begin{pmatrix} \mathbf{u} \\ \dot{\mathbf{u}} \end{pmatrix} \tag{3.33}$$

or

$$\begin{pmatrix} \dot{\mathbf{u}} \\ \ddot{\mathbf{u}} \end{pmatrix} = \begin{bmatrix} \mathbf{0} & \mathbf{I} \\ -\mathbf{M}^{-1}\mathbf{K} & -\mathbf{M}^{-1}\mathbf{C} \end{bmatrix} \begin{pmatrix} \mathbf{u} \\ \dot{\mathbf{u}} \end{pmatrix}. \tag{3.34}$$

Denoting

$$\mathbf{z} = \begin{pmatrix} \mathbf{u} \\ \dot{\mathbf{u}} \end{pmatrix} \tag{3.35}$$

and

$$\mathbf{A} = \begin{bmatrix} \mathbf{0} & \mathbf{I} \\ -\mathbf{M}^{-1}\mathbf{K} & -\mathbf{M}^{-1}\mathbf{C} \end{bmatrix}, \tag{3.36}$$

Equation (3.34) takes the form of (3.25), and the sensitivity of the eigenvalues to the parameters can be determined by (3.29).

The sensitivity analysis process is completed in detail for J. The only matrix that contains J is $\mathbf{M}$. The matrix $\mathbf{M}^{-1}$ takes the form

$$\mathbf{M}^{-1} = \begin{bmatrix} m^{-1} & 0 \\ 0 & J^{-1} \end{bmatrix}. \tag{3.37}$$

Hence by (3.36)

$$\mathbf{A} = \begin{bmatrix} 0 & 0 & 1 & 0 \\ 0 & 0 & 0 & 1 \\ \dfrac{l(k_1+k_2)}{2m} & \dfrac{l(k_2-k_1)}{2m} & \dfrac{l(c_1+c_2)}{2m} & \dfrac{l(c_2-c_1)}{2m} \\ \dfrac{l(k_2-k_1)}{2J} & \dfrac{l^2(k_1+k_2)}{4J} & \dfrac{l(c_2-c_1)}{2J} & \dfrac{l^2(c_1+c_2)}{4J} \end{bmatrix}. \tag{3.38}$$

Therefore,

$$\frac{\partial \mathbf{A}}{\partial J} = \begin{bmatrix} 0 & 0 & 0 & 0 \\ 0 & 0 & 0 & 0 \\ 0 & 0 & 0 & 0 \\ \dfrac{l(k_2-k_1)}{2J^2} & \dfrac{l^2(k_1+k_2)}{4J^2} & \dfrac{l(c_2-c_1)}{2J^2} & \dfrac{l^2(c_1+c_2)}{4J^2} \end{bmatrix}. \tag{3.39}$$

Using MATLAB, $\frac{\partial \lambda_1}{\partial J}$ and $\frac{\partial \lambda_2}{\partial J}$ were determined. Once $\frac{\partial \lambda_1}{\partial J}$ and $\frac{\partial \lambda_2}{\partial J}$ are obtained it is necessary to make sure that the results are correct. In order for this theory to apply, $\frac{\partial \lambda_i}{\partial a_p} \approx da_p$ for small Δa, where $da_p = \frac{s_1 - s_0}{\Delta a}$. s_1 is the new eigenvalue after incremental change, Δa, and s_0 is the original eigenvalue. So for small Δa, $\frac{\partial \lambda_i}{\partial a_p}$ should converge to da_p. Tables 3.4 and 3.5 show the theoretical and approximated sensitivities to the first and second eigenvalues, with $\Delta J = 0.001$.

Table 3.4: Sensitivity Analysis for $\partial\lambda_1 / \partial J$		
ΔJ / l_1	ΔJ=0.001	
	$\partial\lambda_1/\partial J$	dJ
2.53	$(0.00908 + 0.35784i) \times 10^{-3}$	$(0.00908 + 0.35784i) \times 10^{-3}$
2.63	$(0.00779 + 0.31940i) \times 10^{-3}$	$(0.00779 + 0.31940i) \times 10^{-3}$
2.73	$(0.00671 + 0.28619i) \times 10^{-3}$	$(0.00671 + 0.28619i) \times 10^{-3}$
2.83	$(0.00582 + 0.25736i) \times 10^{-3}$	$(0.00582 + 0.25736i) \times 10^{-3}$
2.93	$(0.00507 + 0.23224i) \times 10^{-3}$	$(0.00507 + 0.23224i) \times 10^{-3}$
3.03	$(0.00443 + 0.21025i) \times 10^{-3}$	$(0.00443 + 0.21025i) \times 10^{-3}$

Table 3.5: Sensitivity Analysis for $\partial\lambda_2 / \partial J$		
ΔJ / l_1	ΔJ=0.001	
	$\partial\lambda_2/\partial J$	dJ
2.53	$(0.01240 - 0.96686i) \times 10^{-5}$	$(0.01240 - 0.96686i) \times 10^{-5}$
2.63	$(0.00978 - 0.77239i) \times 10^{-5}$	$(0.00978 - 0.77239i) \times 10^{-5}$
2.73	$(0.00785 - 0.62636i) \times 10^{-5}$	$(0.00785 - 0.62636i) \times 10^{-5}$
2.83	$(0.00639 - 0.51456i) \times 10^{-5}$	$(0.00639 - 0.51456i) \times 10^{-5}$
2.93	$(0.00528 - 0.42754i) \times 10^{-5}$	$(0.00528 - 0.42754i) \times 10^{-5}$
3.03	$(0.00440 - 0.35879i) \times 10^{-5}$	$(0.00440 - 0.35879i) \times 10^{-5}$

It is evident that both $\frac{\partial\lambda_1}{\partial J}$ and $\frac{\partial\lambda_2}{\partial J}$ converge to da_p. The real and imaginary part converges to five decimal places, which is a good approximation. The simulation results are in Figures 3.28 and 3.29.

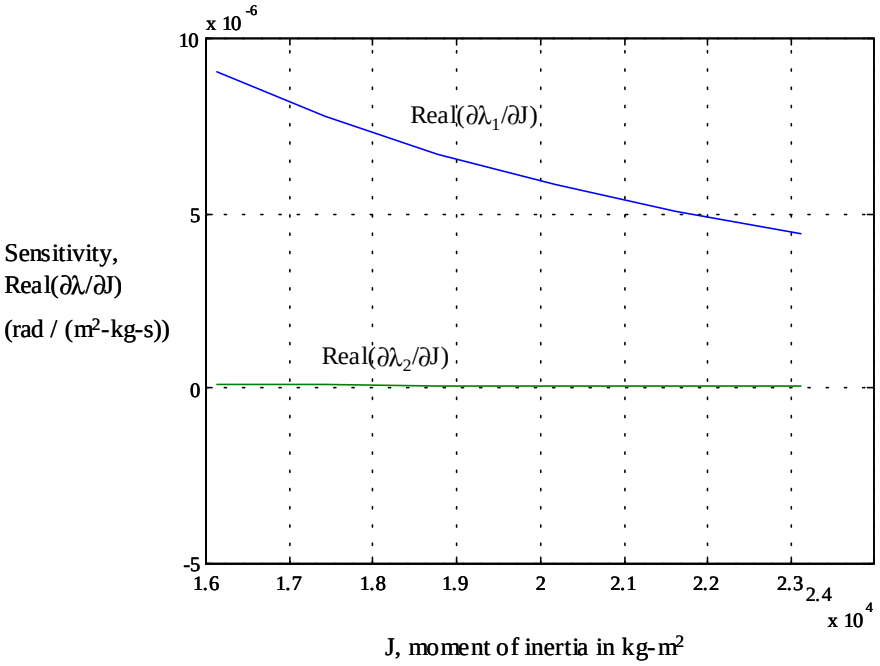

Figure 3.28: Real part of sensitivity of the eigenvalues for both DOF (J)

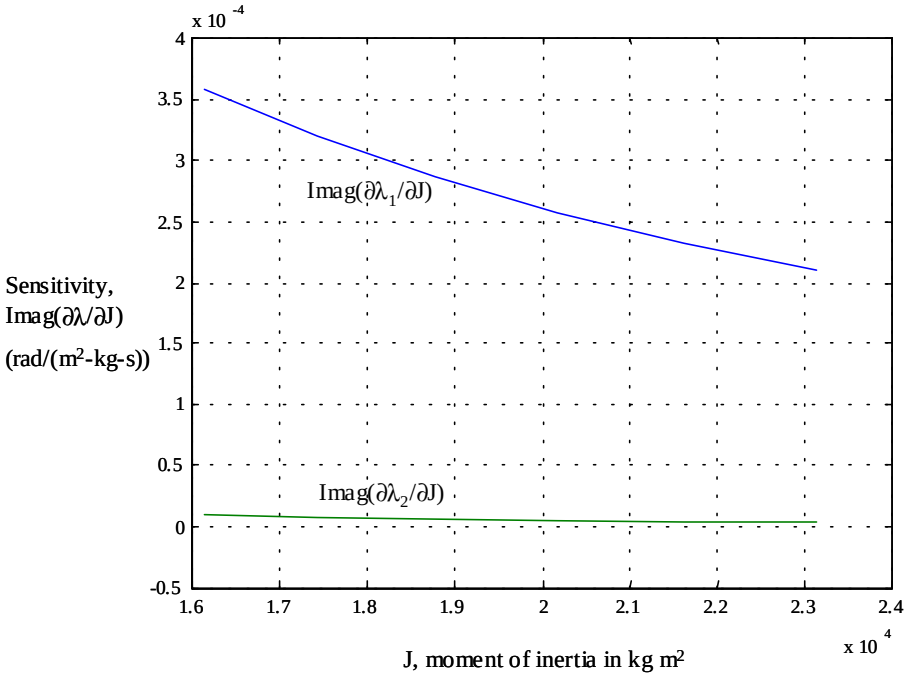

Figure 3.29: Imaginary part of sensitivity of the eigenvalues for both DOF (J)

Figures 3.28 and 3.29 show that as J increases, the sensitivity decreases for the first and second eigenvalue. Although the sensitivity is approximately zero, as shown in the above figures, the first eigenvalue is more sensitive than the second eigenvalue.

The second sensitivity analysis is on m, where

$$\mathbf{A} = \begin{bmatrix} 0 & 0 & 1 & 0 \\ 0 & 0 & 0 & 1 \\ \frac{l(k_1+k_2)}{2m} & \frac{l(k_2-k_1)}{2m} & \frac{l(c_1+c_2)}{2m} & \frac{l(c_2-c_1)}{2m} \\ \frac{l(k_2-k_1)}{2mr^2} & \frac{l^2(k_1+k_2)}{4mr^2} & \frac{l(c_2-c_1)}{2mr^2} & \frac{l^2(c_1+c_2)}{4mr^2} \end{bmatrix} \tag{3.40}$$

and

$$\frac{\partial \mathbf{A}}{\partial m} = \begin{bmatrix} 0 & 0 & 0 & 0 \\ 0 & 0 & 0 & 0 \\ \frac{k_1+k_2}{m^2} & \frac{l(k_2-k_1)}{2m^2} & \frac{c_1+c_2}{m^2} & \frac{l(c_2-c_1)}{2m^2} \\ \frac{l(k_2-k_1)}{2m^2r^2} & \frac{l^2(k_1+k_2)}{4m^2r^2} & \frac{l(c_2-c_1)}{2m^2r^2} & \frac{l^2(c_1+c_2)}{4m^2r^2} \end{bmatrix}. \tag{3.41}$$

The simulation results are shown in Figures 3.30 and 3.31.

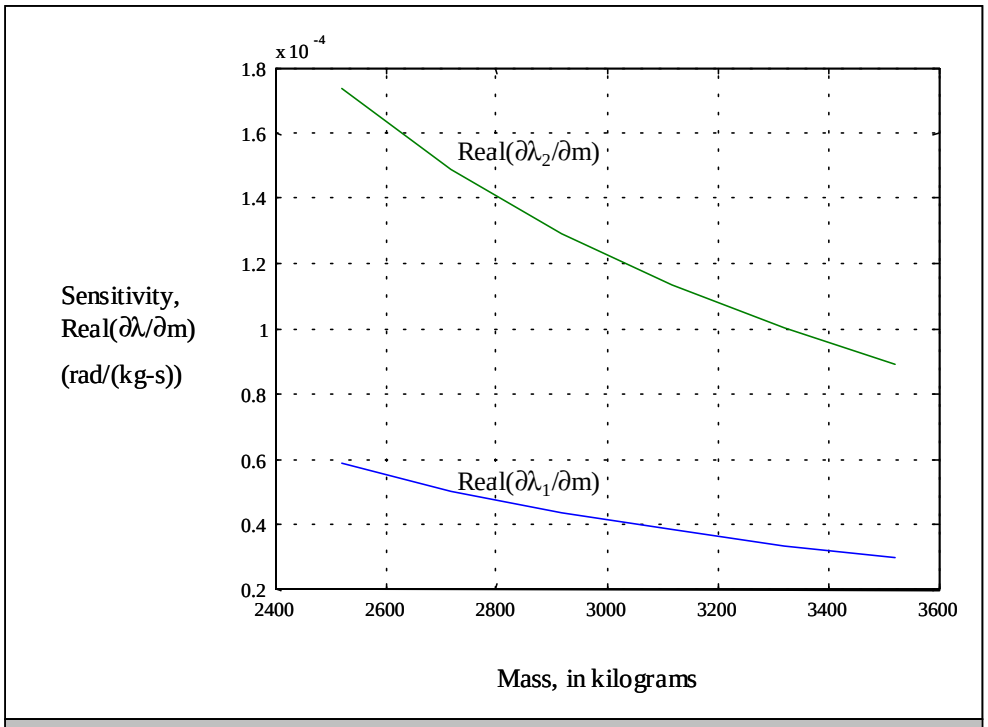

Figure 3.30: Real part of sensitivity of the eigenvalues for both DOF (m)

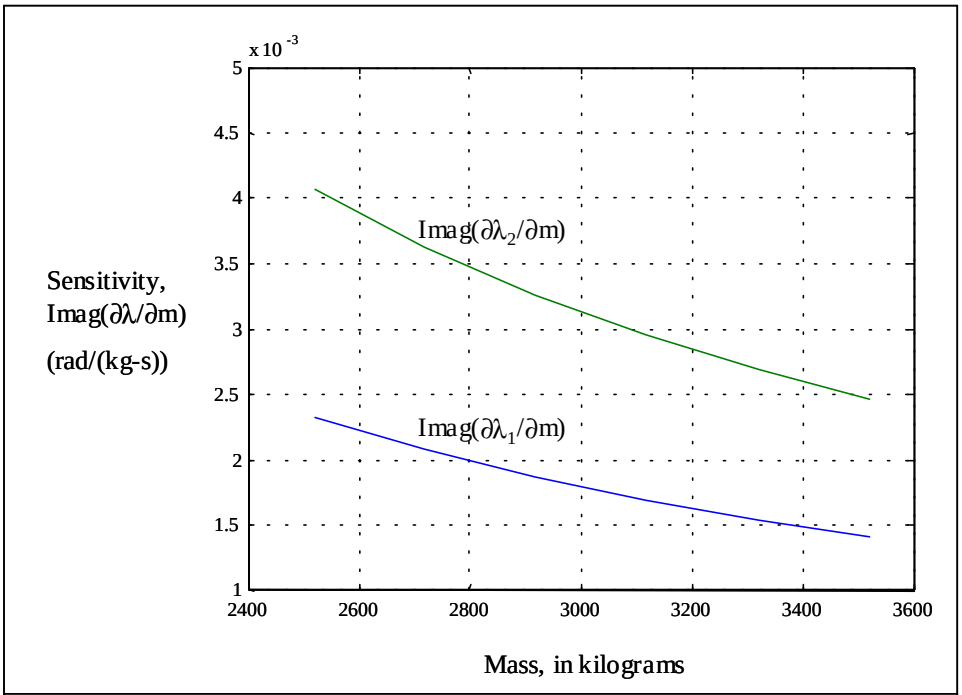

Figure 3.31: Imaginary part of sensitivity of the eigenvalues for both DOF (m)

As the mass increases, the sensitivity of both eigenvalues decreases as in the sensitivity analysis on J. However, although the sensitivity is once again approximately zero, the second eigenvalue is more sensitive than the first eigenvalue.

The third sensitivity analysis is on k_1, where from Equation (3.40)

$$\frac{\partial \mathbf{A}}{\partial k_1} = \begin{bmatrix} 0 & 0 & 0 & 0 \\ 0 & 0 & 0 & 0 \\ m^{-1} & -0.5lm^{-1} & 0 & 0 \\ -0.5lm^{-1} & 0.25l^2m^{-1} & 0 & 0 \end{bmatrix}. \tag{3.42}$$

The simulation results are shown in Figures 3.32 and 3.33.

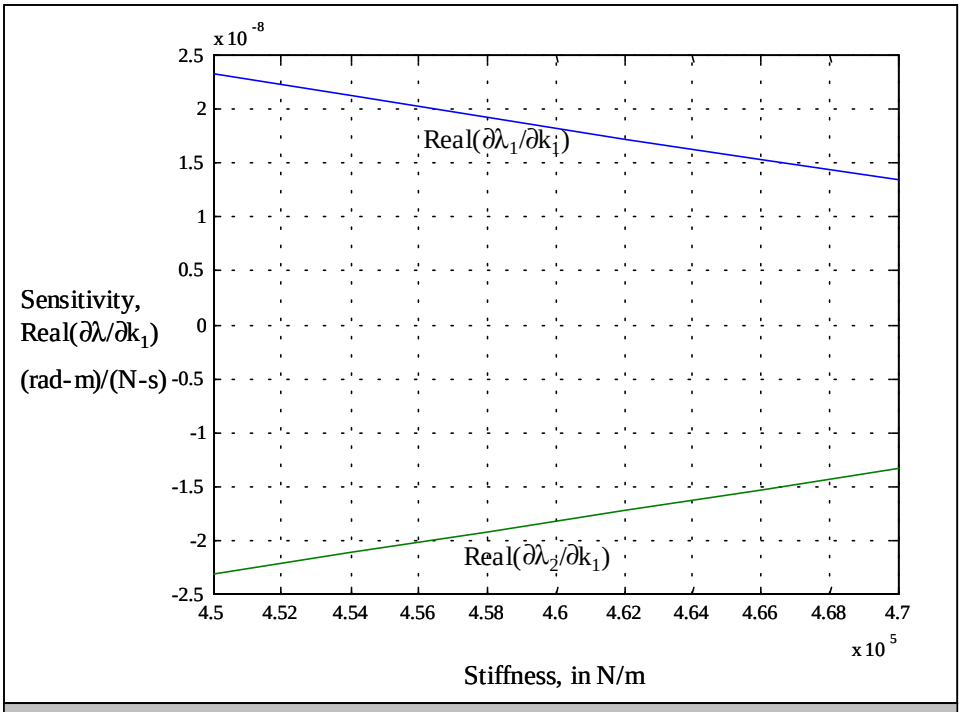

Figure 3.32: Real part of sensitivity of the eigenvalues for both DOF (k_1)

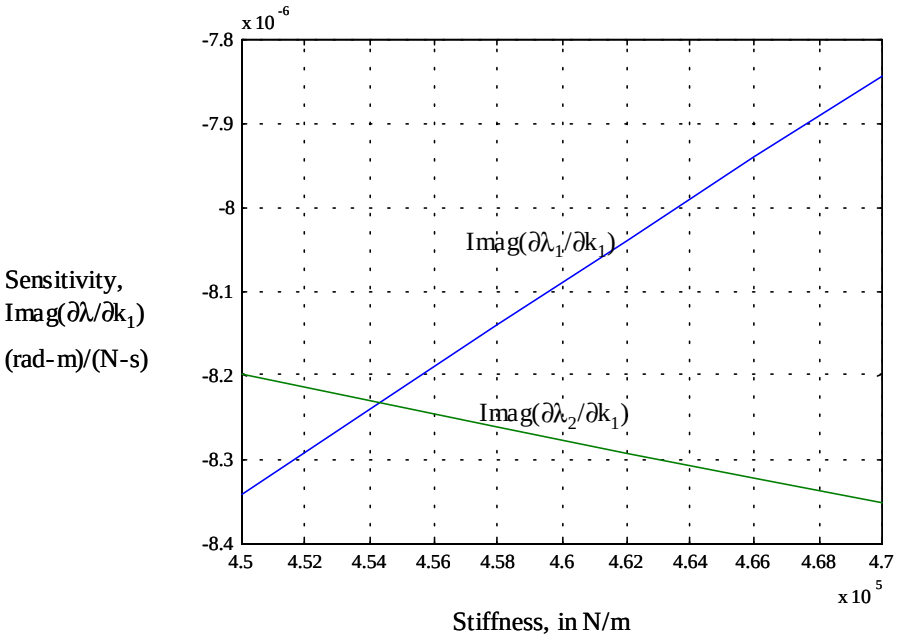

Figure 3.33: Imaginary part of sensitivity of the eigenvalues for both DOF (k_1)

Figures 3.32 and 3.33 indicate that small perturbations in the stiffness have the slightest effect on the sensitivity of the eigenvalues. The simulation results follow for k_2, so it is not necessary to duplicate the graphs.

The fourth sensitivity analysis is on c_1, where

$$\frac{\partial \mathbf{A}}{\partial c_1} = \begin{bmatrix} 0 & 0 & 0 & 0 \\ 0 & 0 & 0 & 0 \\ 0 & 0 & m^{-1} & -0.5lm^{-1} \\ 0 & 0 & -0.5lm^{-1} & 0.25l^2m^{-1} \end{bmatrix}. \tag{3.43}$$

The simulation results are shown in Figures 3.34 and 3.35.

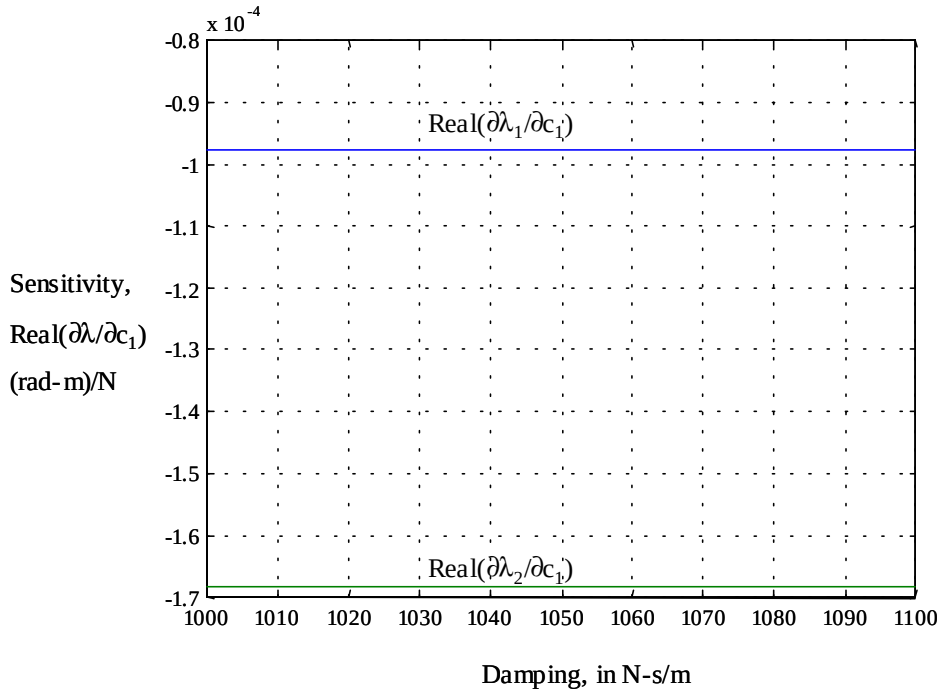

Figure 3.34: Real part of sensitivity of the eigenvalues for both DOF (c_1)

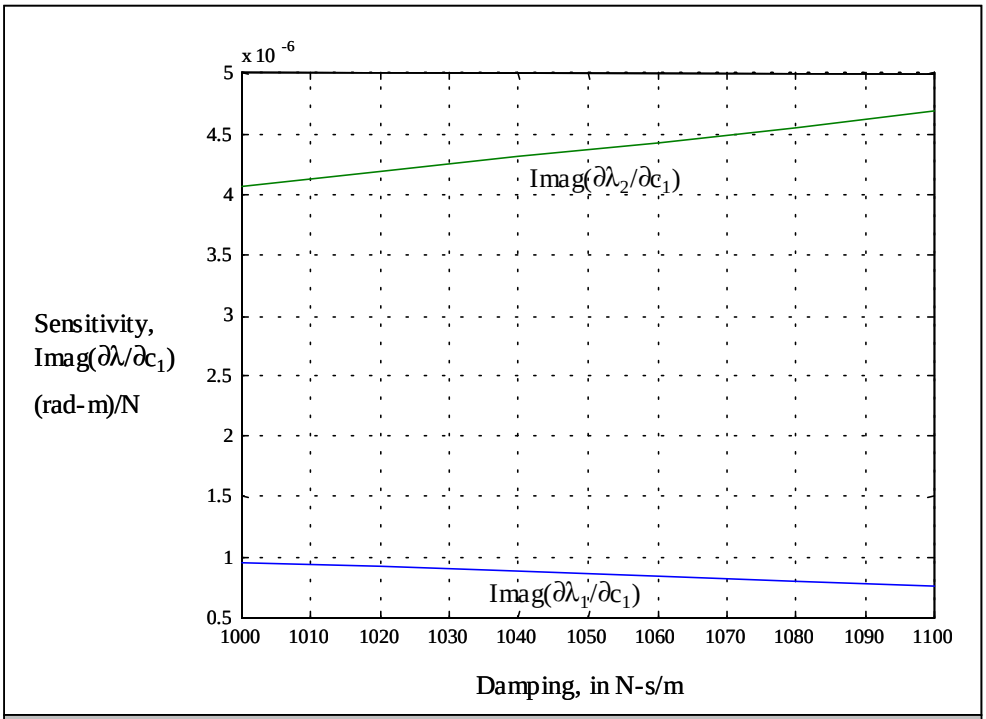

Figure 3.35: Imaginary part of sensitivity of the eigenvalues for both DOF (c_1)

Figure 3.34 shows that as the damping increases, it has no effect on the real part of the sensitivity of the eigenvalue. Figure 3.35 shows that an increase in the damping has a slight effect on the imaginary part of the sensitivity of the eigenvalues, but is still approximately zero. The results follow for c_2 so it is not necessary to duplicate the graphs.

Figures 3.28-3.35 reflect the parametric results in Section 3.3. Recall that the real part of the complex numbers deals with damping and the imaginary part deals with the natural frequencies. The real part of the sensitivity for J, m, k_1, and c_1 is approximately zero indicating the increase in damping has no effect on the system. The imaginary part of the sensitivity, although very small, reflects the increase or decrease in the two damped natural frequencies in Section 3.3. The mass seems to be the most sensitive of all the parameters, although it is extremely small. Recall the parametric analysis on the mass, J was also affected, so it makes sense that the mass would be more sensitive than the other parameters.

CHAPTER 4: EXPERIMENTAL VERIFICATION

4.1 Introduction

The objective here is to be able to implement the theory in practical applications. This chapter deals with a laboratory experiment, imitating the configuration in Figure 3.1, carried out in order to validate the method developed and results derived. However, the experiment is a free vibration experiment and excludes damping. There will be two parts to the experimental validation. The first will be results based on the experimental setup. The second part of this chapter is based on the analytical results and then both of these results will be compared.

4.2 Experimental Determination

Modal testing is used to obtain the natural frequencies for the experimental setup. Modal testing is a test where the structure or component is vibrated with a known excitation, most times out of its normal service environment, which includes both the data acquisition, and its subsequent analysis. Below is a description of the equipment, setup, procedure for each test and results.

4.2.1 Equipment

A quartz shear ICP accelerometer, Model 353B33, from PCB Piezotronic is used in the experimental setup. The accelerometer has a frequency range of 2 Hz to 4000 Hz. An Impact Hammer, Model 291M78-086C05 made by PCB Piezotronics, causes the impact during the experiment. The striking end of the hammerhead consists of an integral ICP quartz force sensor. The frequency range for this sensor is 5 kHz and the

hammer range is 22000N. The ICP power to the accelerometer and the hammer are supplied by the BNC 2140 from National Instruments. The BNC 2140 connects the accelerometer and hammer to the computer by way of a data collection system. The data collection system used consisted of a NI 4551 PCI-based Dynamic Signal Analyzer (DSA) Instrument and the software Virtual Work Bench by National Instruments. The NI 4551 is specifically designed to make high-accuracy measurements. With the Virtual Work Bench DSA software, many measurements can be performed such as the power spectrum, cross power spectrum, and frequency response. This software has several views, simultaneous displays, and averaging methods that can be used when measuring the vibration in a system.

4.2.2 Setup

The complete setup is shown in Figure 4.1. When designing this experiment, there were several issues to consider. (1) System must be rigid. (2) When springs deform, they must deform linearly. (3) Mass should be heavy enough to cause deformation. (4) Best to design system in such a way that each parameter can be perturbed without much complication. (4) Make sure setup has a firm base to prevent movement during testing. (5) Mount accelerometer securely to the structure to avoid relative motion between the accelerometer and the structure. (6) Carefully consider the placement of the accelerometer to obtain the best results. (7) Make sure that the impact of the hammer is quick and sharp.

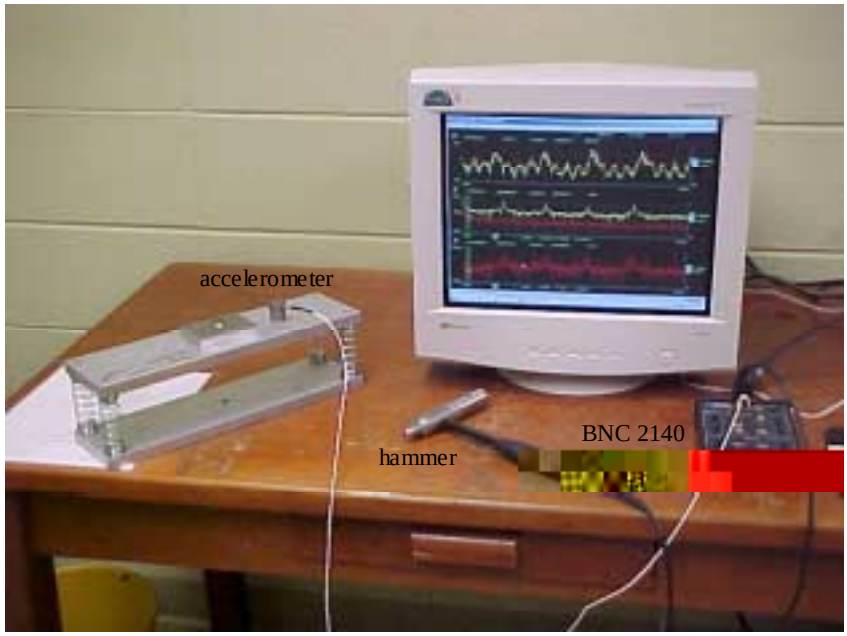

Figure 4.1: Complete experimental setup

4.2.3 Procedure

The procedure has three parts to it. For the first part, the base system in Figure 4.2, is placed on the floor for steady support. The accelerometer was attached to the top plate using double-sided tape. The accelerometer was attached as close as possible to the center of gravity, but allowing enough space to modify the experiment for testing of other parameters. The system was then hit with the impact hammer and the data was recorded. Before recording, the system was hit several times to be sure that the results were repeatable.

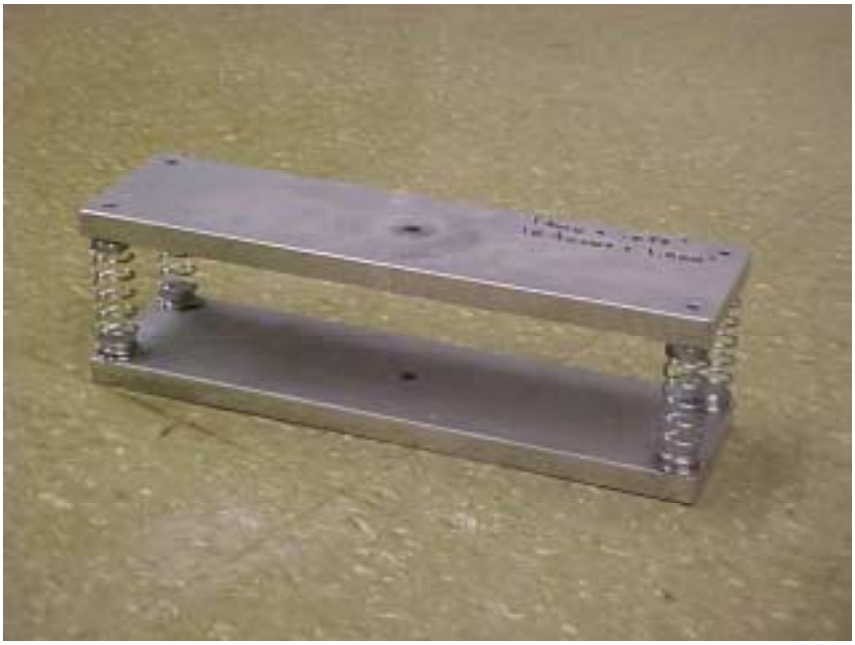

Figure 4.2: 2-DOF mass-spring system

For Part two of this procedure, two masses were used in this part of the experiment. The first small mass was attached to the base system at the center of gravity as in Figure 4.3. The system was hit several times with the impact hammer to make sure the data was repeatable and then the data was recorded. The first mass was removed and then the second mass was added. The system was hit again several times and then the data was recorded.

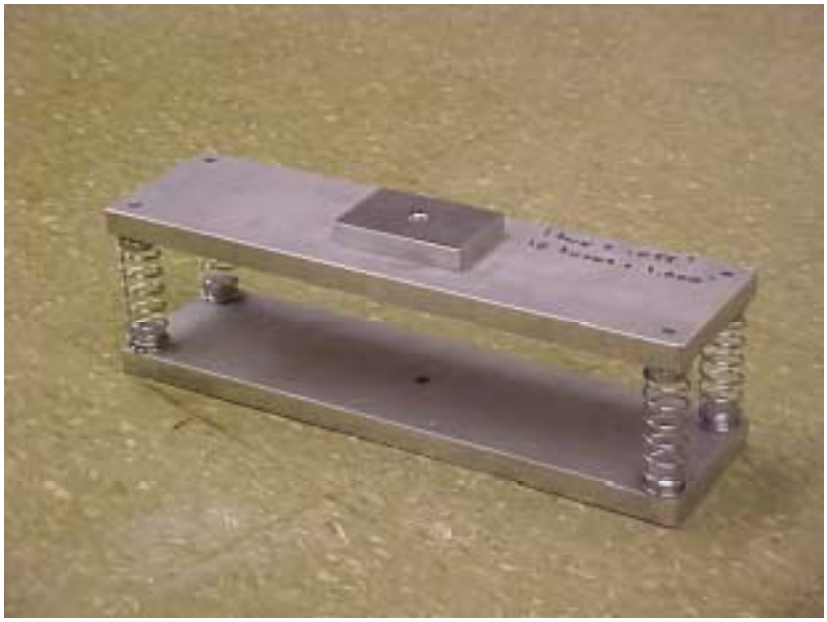

Figure 4.3: 2-DOF mass-spring system with added mass

For Part 3 of this procedure, all pieces added to the base system in the previous testing were removed. Two springs were used in this part of the experiment. The first was attached at the center of gravity by using a rod and knob as shown in Figures 4.4 and 4.5. The knob compresses the top plate down to the height of the center spring. The system was then tested as in the previous experiments and the data was recorded. The second spring was then tested and the data was recorded. All results are seen in the next section.

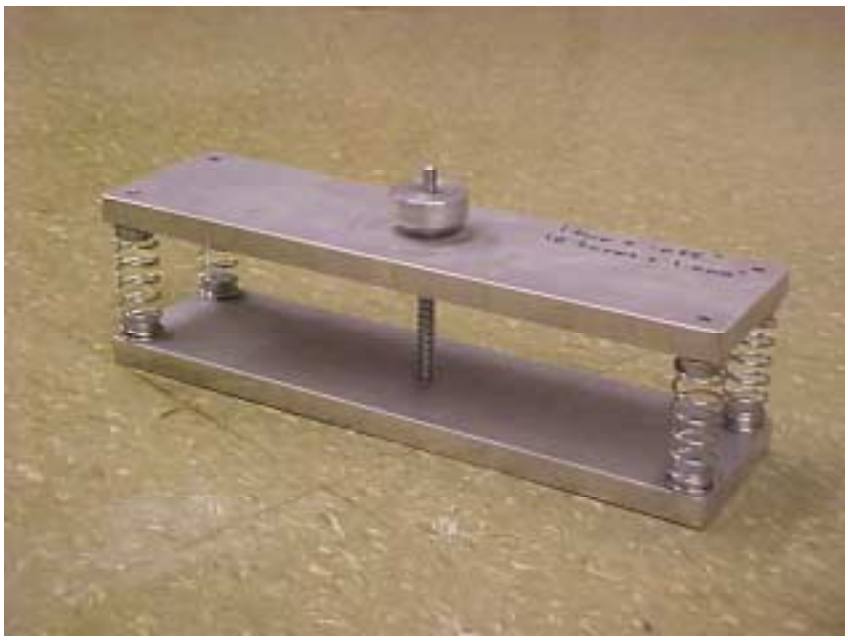

Figure 4.4: 2-DOF mass-spring system with stiffness modification

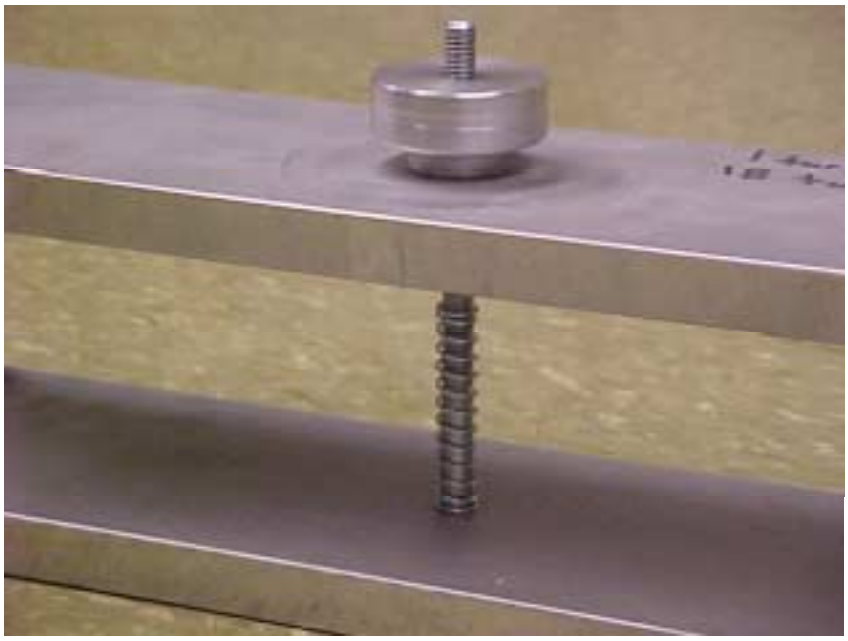

Figure 4.5: Close-up of mass-spring system modification

4.2.4 Results

This section displays the results obtained from using the described equipment in Section 4.2.1. Figure 4.6 is a snap shot of the results for the system in Figure 4.2. The first display is the time waveform of the accelerometer and the hammer, the second display is the amplitude spectrum, and the third display is the transfer function. The data in yellow (top waveform in display 2) represents the output of the accelerometer and the data in red (bottom waveform in display 2) represents the output of the hammer. The peaks seen in the second display represent the natural frequencies of the system. The first natural frequency is at 12.06 Hz and the second natural frequency is at 24.06 Hz. These results are fairly close to what was predicted earlier in the analytical determination. However, there are more than two natural frequencies seen in this figure. This means that although only 2-DOF are represented in the mathematical model, the actual setup has more DOF than what is being investigated.

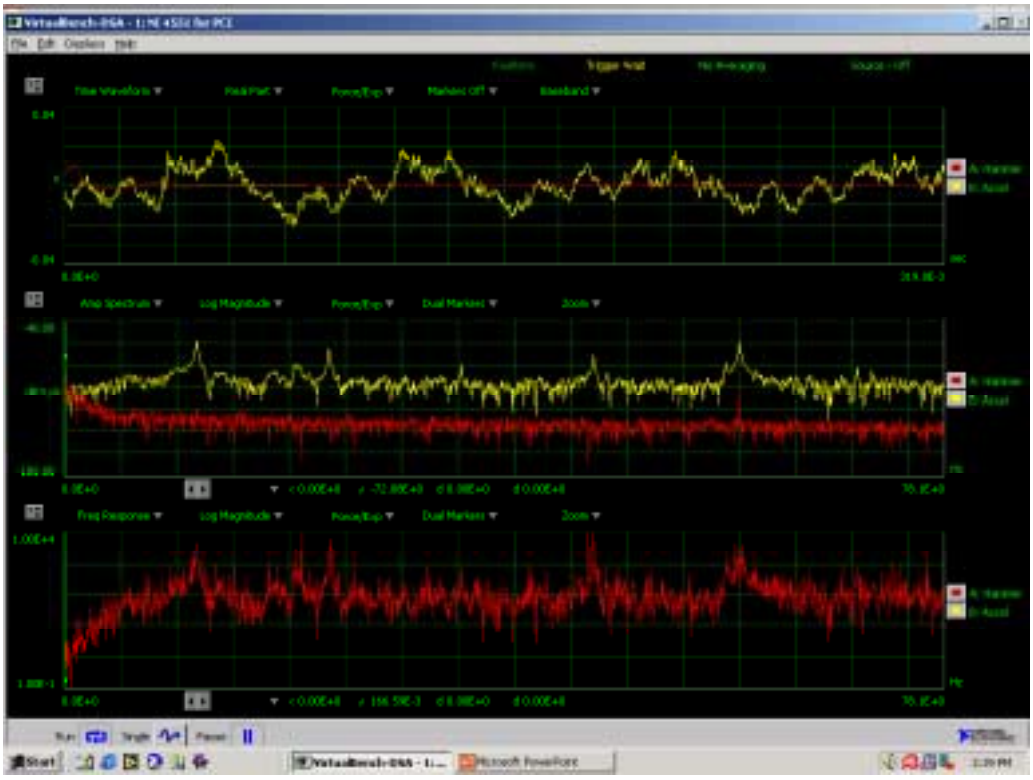

Figure 4.6: Results for mass-spring system

For Figure 4.3, when $m_1 = 0.063\ kg$, the experimental results are shown in Figure 4.7. The first natural frequency is at 11.87 Hz and the second natural frequency is at 23.54 Hz.

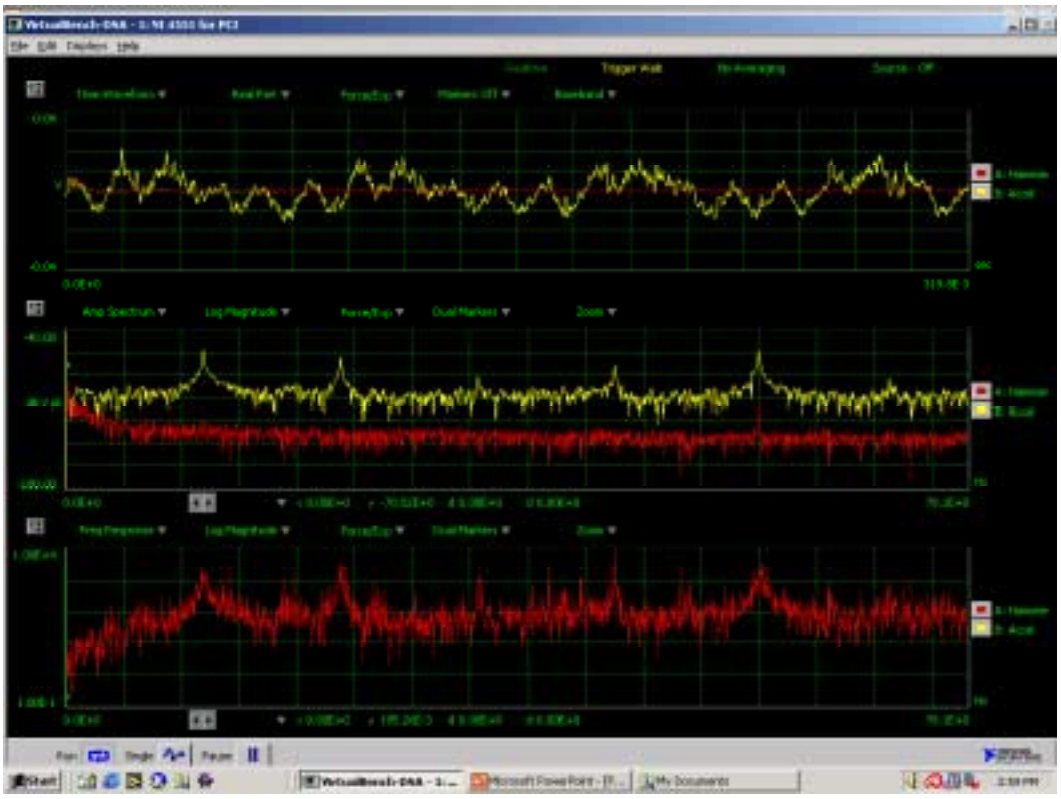

Figure 4.7: Snap shop results for added mass, m_1=0.063 kg

For the second added mass, $m_2 = 0.122\ kg$, and the experimental results are shown in Figure 4.8. The first natural frequency is at 11.77 Hz and the second natural frequency is at 23.44 Hz.

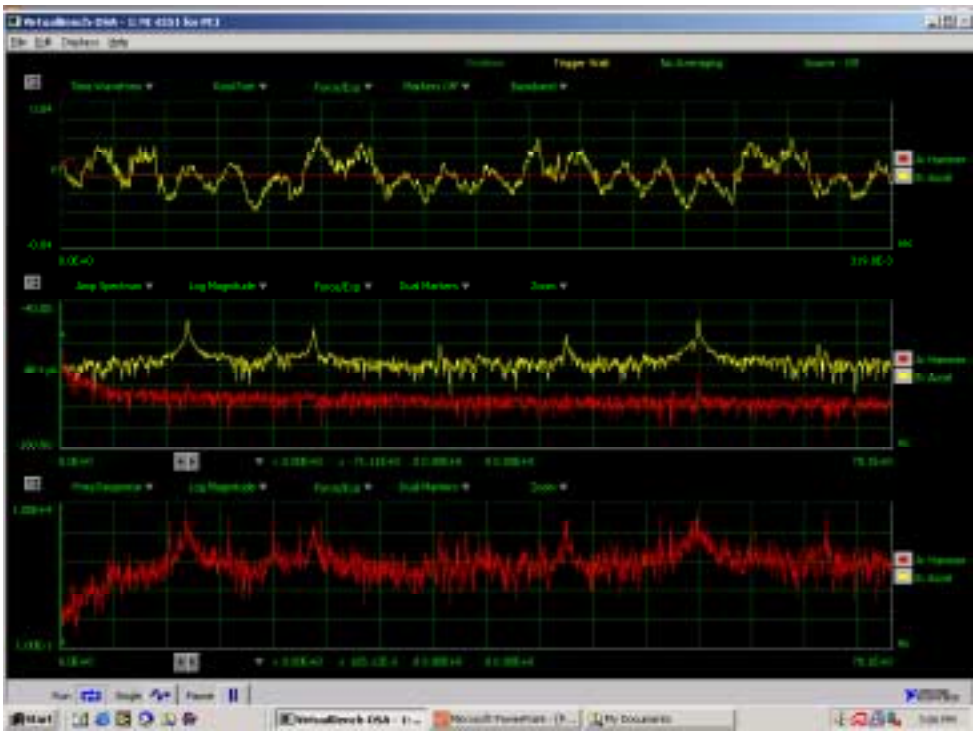

Figure 4.8: Snap shot results for added mass, m_2=0.122 kg

For Figure 4.4 and 4.5, when $k_3 = 910.7 \frac{N}{m}$ the experimental results are shown in Figure 4.9. In display two, the first natural frequency is at 12.06 Hz and the second natural frequency is at 24.06 Hz.

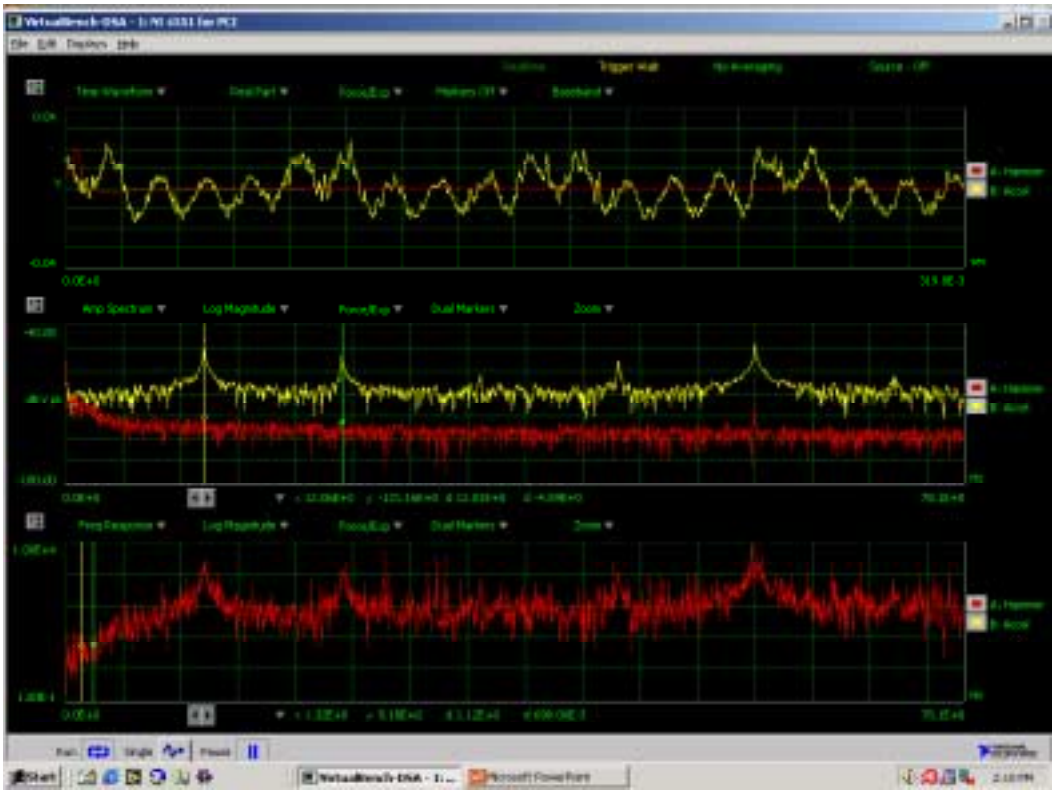

Figure 4.9: Snap shot results for mass-spring system, k_3=910.7 N/m

When $k_3 = 1313 \frac{N}{m}$ the results are shown in Figure 4.10. In display two, the first natural frequency is at 12.06 Hz and the second natural frequency is at 24.06 Hz.

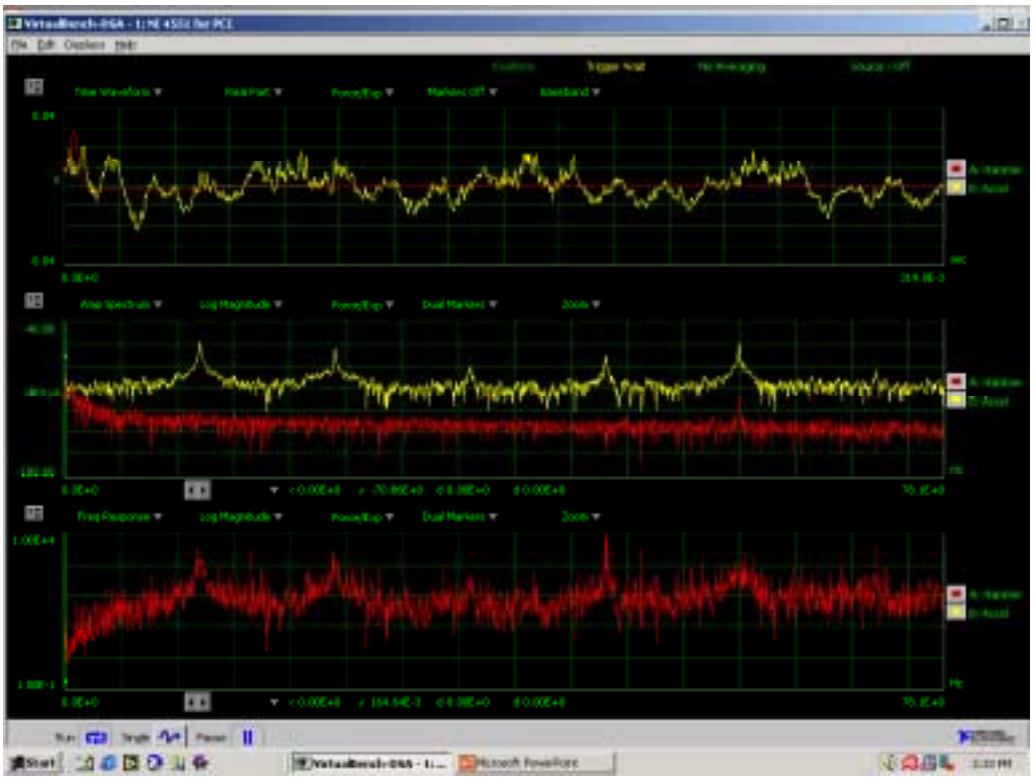

Figure 4.10: Snap shot results for mass-spring system, k_3=1313 N/m

The experimental sensitivity of the eigenvalues can be determined by the following formula:

$$\frac{\Delta\omega_i}{\Delta a_k}\times 2\pi \quad i=1,2,...,n \qquad k=1,2,...,n\,, \tag{4.1}$$

where a_k is any parameter of the system and i represents the number of frequencies in the system. The same two parameters investigated for the parametric analysis will be investigated here as well. The first parameter that will be looked at is the mass. For $m_1 = 0.063\ kg$, Equation (4.1) becomes

$$\frac{\Delta\omega_1}{\Delta m_1} = \frac{11.87-12.06}{0.063}\times 2\pi = -18.949\ \frac{rad-kg}{s} \tag{4.2}$$

and

$$\frac{\Delta\omega_2}{\Delta m_1} = \frac{23.54 - 24.06}{0.063} \times 2\pi = -51.861 \ \frac{rad - kg}{s}. \tag{4.3}$$

For $m_2 = 0.122 \ kg$, Equation (4.1) becomes

$$\frac{\Delta\omega_1}{\Delta m_2} = \frac{11.77 - 12.06}{0.122} \times 2\pi = -14.935 \ \frac{rad - kg}{s} \tag{4.4}$$

and

$$\frac{\Delta\omega_2}{\Delta m_2} = \frac{23.44 - 24.06}{0.122} \times 2\pi = -31.931 \ \frac{rad - kg}{s} \tag{4.5}$$

The second parameter that was looked at was the stiffness. For $k_3 = 910.7 \ N/m$, Equation (4.1) becomes

$$\frac{\Delta\omega_1}{\Delta k_3} = \frac{12.06 - 12.06}{910.7} \times 2\pi = 0.0 \ \frac{rad - m}{N - s} \tag{4.6}$$

and

$$\frac{\Delta\omega_2}{\Delta k_3} = \frac{24.06 - 24.06}{910.7} \times 2\pi = 0.0 \ \frac{rad - m}{N - s}. \tag{4.7}$$

For $k_3 = 1313 \ N/m$, Equation (4.1) becomes

$$\frac{\Delta\omega_1}{\Delta k_3} = \frac{12.06 - 12.06}{1313} \times 2\pi = 0.0 \ \frac{rad - m}{N - s} \tag{4.8}$$

and

$$\frac{\Delta\omega_2}{\Delta k_3} = \frac{24.06 - 24.06}{1313} \times 2\pi = 0.0 \ \frac{rad - m}{N - s} \tag{4.9}$$

4.3 Analytical Determination

The analytical determination consists of the vibration, parametric and sensitivity analysis based on the theory.

4.3.1 Vibration Analysis

In this case, $k_1 = k_2 = 2649\ \frac{N}{m}$. The mass, m, is an aluminum plate with dimensions $0.36\ m \times 0.1\ m \times 0.016\ m$. Aluminum has a density of $2699\ \frac{kg}{m^3}$ and the volume of the plate is $0.0005812\ m^3$. Knowing the volume and density of the aluminum plate, the mass can be calculated and is $1.569\ kg$. Since the mass is a thin aluminum plate, $J = \frac{1}{12} m b^2$, where $b = 0.36\ m$. With no damping in the system, and $k_1 = k_2$, Equation (3.5) reduces to

$$\begin{bmatrix} m & 0 \\ 0 & J \end{bmatrix} \begin{pmatrix} \ddot{u} \\ \ddot{\theta} \end{pmatrix} + \begin{bmatrix} 4k_1 & 0 \\ 0 & k_1 l^2 \end{bmatrix} \begin{pmatrix} u \\ \theta \end{pmatrix} = \begin{pmatrix} 0 \\ 0 \end{pmatrix} \tag{4.10}$$

Substituting in the values, Equation (4.10) becomes

$$\begin{bmatrix} 1.569 & 0 \\ 0 & 0.01695 \end{bmatrix} \begin{pmatrix} \ddot{u} \\ \ddot{\theta} \end{pmatrix} + \begin{bmatrix} 10160 & 0 \\ 0 & 329.18 \end{bmatrix} \begin{pmatrix} u \\ \theta \end{pmatrix} = \begin{pmatrix} 0 \\ 0 \end{pmatrix} \tag{4.11}$$

and the natural frequencies are 12.81 Hz and 22.16 Hz.

4.3.2 Parametric analysis

In order to validate the theory for the parametric analysis, Figure 4.1 is modified as shown in Figures 4.3, 4.4 and 4.5. Two parametric analyses will be performed, (1) mass and (2) stiffness.

(1) Mass

Adding smaller aluminum plates to the base system will perform the parametric analysis for the mass. By doing this, J will also be changed. There are two separate masses, represented as small aluminum plates that will be used for this analysis. The first

plate has dimensions $0.07\ m \times 0.04\ m \times 0.01\ m$, giving it a mass, m_1, of $0.063\ kg$. The moment of inertia of this plate is $0.000023\ kg-m^2$. The second plate has dimensions $0.08\ m \times 0.05 m \times 0.01\ m$, giving it a mass, m_2, of $0.122\ kg$. The moment of inertia of this plate is $0.000064\ kg-m^2$. For m_1, Equation (4.10) becomes

$$\begin{bmatrix} 1.632 & 0 \\ 0 & 0.01763 \end{bmatrix} \begin{pmatrix} \ddot{u} \\ \ddot{\theta} \end{pmatrix} + \begin{bmatrix} 10160 & 0 \\ 0 & 329.18 \end{bmatrix} \begin{pmatrix} u \\ \theta \end{pmatrix} = \begin{pmatrix} 0 \\ 0 \end{pmatrix} \tag{4.12}$$

and the natural frequencies are 12.56 Hz and 21.75 Hz. For m_2, Equation (4.10) becomes

$$\begin{bmatrix} 1.691 & 0 \\ 0 & 0.01826 \end{bmatrix} \begin{pmatrix} \ddot{u} \\ \ddot{\theta} \end{pmatrix} + \begin{bmatrix} 10160 & 0 \\ 0 & 329.18 \end{bmatrix} \begin{pmatrix} u \\ \theta \end{pmatrix} = \begin{pmatrix} 0 \\ 0 \end{pmatrix} \tag{4.13}$$

and the natural frequencies are 12.35 Hz and 21.37 Hz.

(2) Stiffness

The parametric analysis on the stiffness, k_1, will be performed by changing the stiffness parameter, k_3 shown in Figure 4.4 and 4.5. The values for k_3 are 910.7 $\frac{N}{m}$ and 1313 $\frac{N}{m}$. For $k_3 = 910.7\ \frac{N}{m}$, Equation (4.10) becomes

$$\begin{bmatrix} 1.569 & 0 \\ 0 & 0.01698 \end{bmatrix} \begin{pmatrix} \ddot{u} \\ \ddot{\theta} \end{pmatrix} + \begin{bmatrix} 11070.66 & 0 \\ 0 & 329.18 \end{bmatrix} \begin{pmatrix} u \\ \theta \end{pmatrix} = \begin{pmatrix} 0 \\ 0 \end{pmatrix} \tag{4.14}$$

and the natural frequencies are 13.37 Hz and 22.16 Hz. For $k_3 = 1313\ \frac{N}{m}$, Equation (4.10) becomes

$$\begin{bmatrix} 1.569 & 0 \\ 0 & 0.01698 \end{bmatrix} \begin{pmatrix} \ddot{u} \\ \ddot{\theta} \end{pmatrix} + \begin{bmatrix} 11473.45 & 0 \\ 0 & 329.18 \end{bmatrix} \begin{pmatrix} u \\ \theta \end{pmatrix} = \begin{pmatrix} 0 \\ 0 \end{pmatrix} \tag{4.15}$$

and the natural frequencies are 13.61 hz and 22.16 hz.

Table 4.1 shows a comparison between the experimental and analytical parametric analysis.

Table 4.1: Experimental and analytical parametric analysis results

	Base system		m_1=0.122 kg		m_2=0.063 kg		k_3=910.66 N/m		k_3=1313.45 N/m	
ω_n	Exp	Analy	Exp	Analy	Exp	Analy	Exp	Analy	Exp	Analy
1	12.06	12.81	11.87	12.56	11.77	12.35	12.06	13.37	12.06	13.61
2	24.06	22.16	23.54	21.75	23.44	21.37	24.06	22.16	24.06	22.16

From Table 4.1, the mass-spring system design seemed to be a good way to verify the theory because there was a minimum error of 4.9% and a maximum error of 12.9%. However, just how good these results are will be better determined from the sensitivity analysis.

4.3.3 Sensitivity Analysis

Following from the parametric analysis, the sensitivity of the parameters to perturbations can be determined. Two sensitivity analyses will be performed, (1) mass and (2) stiffness.

(1) Mass

Following the sensitivity analysis from Section 3.4.2, Equation (3.36) becomes

$$\mathbf{A} = \begin{bmatrix} 0 & 0 & 1 & 0 \\ 0 & 0 & 0 & 1 \\ m^{-1}k_1 & 0 & 0 & 0 \\ 0 & J^{-1}k_1 & 0 & 0 \end{bmatrix} \tag{4.16}$$

therefore,

$$\frac{\partial \mathbf{A}}{\partial m} = \begin{bmatrix} 0 & 0 & 0 & 0 \\ 0 & 0 & 0 & 0 \\ -k_1 m^{-2} & 0 & 0 & 0 \\ 0 & -12(mb)^{-2} & 0 & 0 \end{bmatrix} \tag{4.17}$$

Using MATLAB, $\frac{\partial \lambda_1}{\partial m}$ and $\frac{\partial \lambda_2}{\partial m}$ were determined. The results are shown in Figures 4.11. Only the imaginary part of the sensitivity is shown because the real part is zero indicating there is no damping in the system.

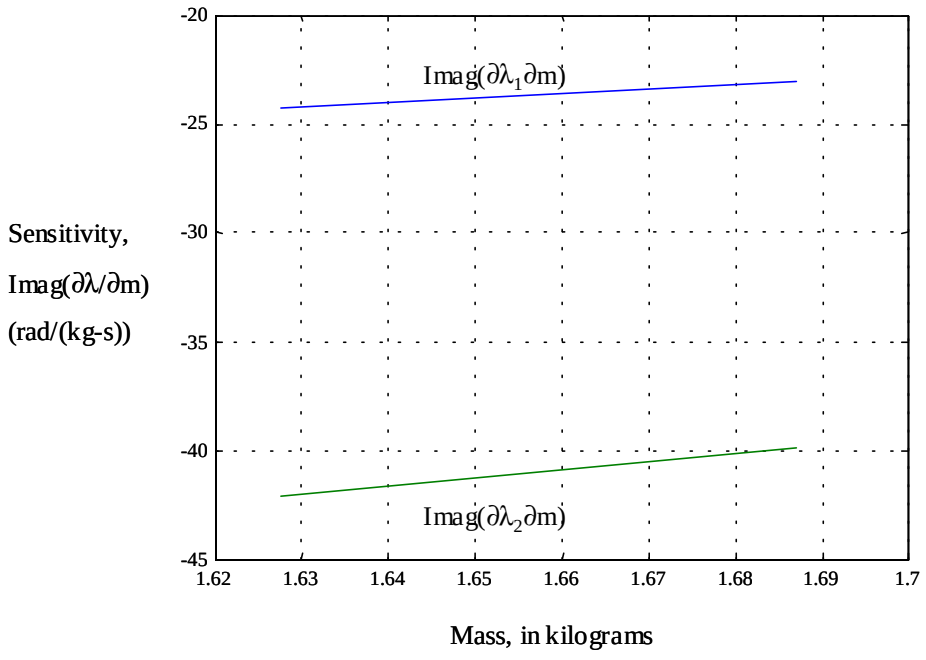

Figure 4.11: Experiment-imaginary part of sensitivity for both DOF (mass)

(2) Stiffness

Following the sensitivity analysis from Section 3.4.2, Equation (3.36) becomes

$$\frac{\partial \mathbf{A}}{\partial k_1} = \begin{bmatrix} 0 & 0 & 0 & 0 \\ 0 & 0 & 0 & 0 \\ m^{-1} & 0 & 0 & 0 \\ 0 & J^{-1} & 0 & 0 \end{bmatrix}. \tag{4.18}$$

Using MATLAB, $\frac{\partial \lambda_1}{\partial k_1}$ and $\frac{\partial \lambda_2}{\partial k_1}$ were determined. The results are shown in Figure 4.12. Only the imaginary part of the sensitivity of the first eigenvalue is seen because the second eigenvalue is zero.

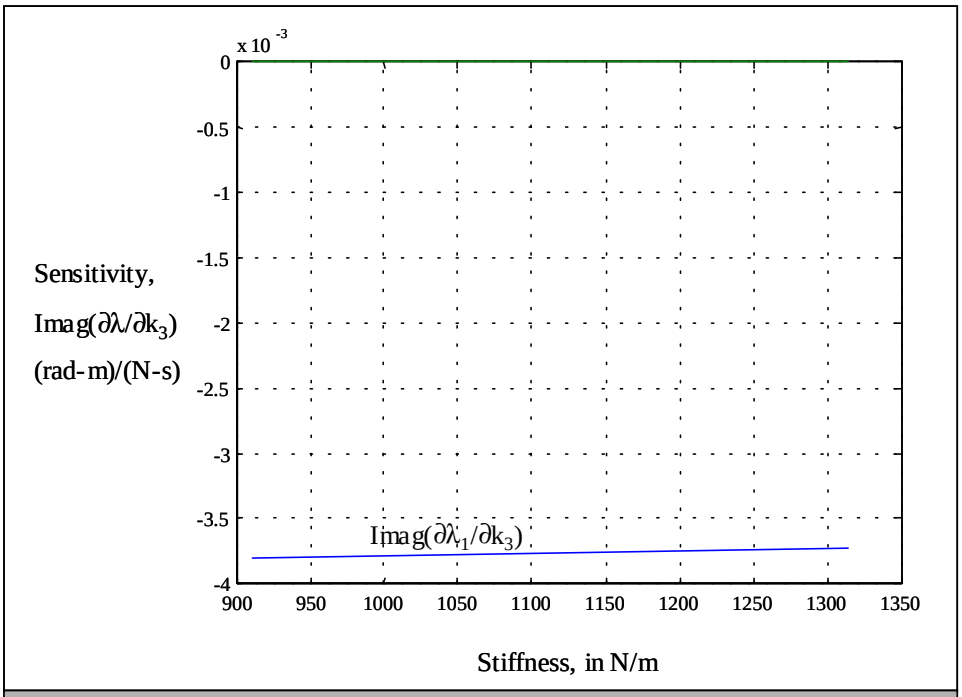

Figure 4.12: Experiment-imaginary part of sensitivity for both DOF (k_3)

Table 4.2 shows comparison between the experimental and sensitivity analysis results.

Table 4.2: Experimental and analytical sensitivity analysis results								
	m_1=0.063 kg		m_2=0.122 kg		k_3=910.7 N/m		k_3=1313 N/m	
$\partial\lambda/\partial a_i$	Exp	Analy	Exp	Analy	Exp	Analy	Exp	Analy
1	-18.949i	-24.2713i	-14.935i	-23.0006i	0	-0.0038i	0	-0.0037i
2	-51.861i	-42.0392	-31.931i	-39.8383i	0	0	0	0

Table 4.2 shows that the error ranges from 28.09-54.0% and 18.94-24.76% for the sensitivities on the first and second eigenvalue, respectively, with mass incremental changes. This error is high because the mass in this case is a very sensitive parameter, so the slightest change affects it drastically. The Virtual Work Bench software used in this experiment has cursors that aid in helping to find the value of the peaks or natural frequencies, as in Figures 4.6-4.10. For example, if

$$\frac{\Delta\omega_1}{\Delta m_2} = \frac{11.78 - 12.06}{0.122} \times 2\pi = -13.91 \, \frac{rad - kg}{s}$$

or

$$\frac{\Delta\omega_1}{\Delta m_2} = \frac{11.57 - 12.06}{0.122} \times 2\pi = -25.24 \, \frac{rad - kg}{s},$$

the error in sensitivity can increase to 65.35% or decrease to 8.87% from the original 54.0%. Therefore, this high error is due to error in experimental measurements that are not seen by the human eye. It is evident that the best results were obtained for the stiffness for the first and second eigenvalue.

CONCLUSION AND RECOMMENDATIONS

5.1 Conclusion

Vibration analysis is an inherent part of the design of any mechanical system. The work done in this thesis was to develop a parametric and sensitivity methodology for the effects of vibration in an automobile. Several supporting articles were given which cover several techniques that others have proposed and implemented, in order to reduce the vibration response of the system. This is essential because an increase in vibration causes an undesirable effect for the driver.

A literature survey of past work was provided in developing a mathematical model to best determine the vibration response in vehicle system modeling, vehicle structure modes, tire properties and vehicle handling. The fundamental theory for free and forced vibration for a damped system and the parametric and sensitivity analyses have been provided. From the parametric analysis, J had an effect on the first damped natural frequency only in the bounce mode; but in the pitch mode, J had an effect on magnitude and position of the first damped natural frequency and an effect on the magnitude for the second damped natural frequency. The mass had an effect on both the position and magnitude of both damped natural frequencies in the bounce and pitch mode. Surprisingly, k_1 did not have much of an effect on either of the damped natural frequencies in the bounce or pitch mode. This could be due to the fact that k_1 may not have had a high enough perturbation when compared to k_2. Another reason could be that it was excessively large when compared to the mass, which with a slight change in stiffness and the mass is constant; there was not much difference. The results for c_1

concluded that the damping had no effect on the system because the damping ratio was very close to zero; therefore, $w_d \cong w_n$ and w_n depends only on m and k. For the sensitivity analysis, the mass is the most sensitive parameter. This is mostly evident because when m is changed J is changed as well. The opposite is not true because J can be changed without changing m by changing the dimensions.

The equipment used for the experiment consisted of a quartz shear ICP accelerometer, an impact hammer, DSA Instrument, and the software Virtual Work Bench by National Instruments. This equipment proved successful in the experiment because it allowed for different types of data collection without complication. The natural frequencies obtained from the experiment were fairly close to the natural frequencies obtained analytical. However, although the experimental sensitivities for the most part were close in numbers to the analytical sensitivities, they were not close enough because the error ranged from 0-54%. This large range of error was due to the incremental change in the mass. The larger errors were due the sensitivity on the second eigenvalue. This could be due to the fact that the mass is a sensitive parameter, which was established in the parametric results. Therefore, the mass parameter must be handled with special attention.

5.2 Recommendations for Future Research

There are several issues to consider for further investigation. (1) Investigating the roll mode of the vehicle. (2) Analyzing the system as a lumped mass system, 1-mass and 1-spring. (3) Extend to a realistic automobile by adding more DOF. (4) Include damping in the experiment. (5) Include a harmonic excitation force. (6) Include a vibration absorber in the experiment.

REFERENCES

1. Chrstos, Jeffrey P., "A Simplified Method for the Measurement of Composite Suspension Parameters", SAE Paper 910232, presented at International Congress and Exposition, Detroit, MI, February 25-March 1. 1991.

2. Mimuro, Tetsushi, Masayoshi Ohsaki, Hiromichi Yasunaga and Kohji Satoh, "Four Parameter Evaluation Method of Lateral Transient Response", SAE Paper 901734, presented at Passenger Car Meeting and Exposition, Dearborn, MI, September 17-20, 1990.

3. Hovarth, Jack K., "Structural and System Models", SAE Paper 750135, 1975.

4. Davis, James C., "Modal Modeling Techniques for Vehicle Shake Analysis", SAE Paper 720045, Presented at the Automobile Engineering Congress, Detroit, MI, January 10-14, 1972.

5. Speckhart, Frank H., "A Computer Simulation for Three-Dimensional Vehicle Dynamics", SAE Paper 730526, 1973.

6. Simic, Dusan P. and Zika Petronijevic, "Experimental Analysis of Automobile Body Vibration Characteristics", SAE Paper 861261, presented at the International Off-Highway Powerplant Congress and Exposition, Milwaukee, Wisconsin, September 8-11, 1986.

7. Daberkow, A. and E.J. Kreuzer, "An Integrated Approach for Computer Aided Design in Multibody System Dynamics", *Engineering with Computers*, Vol 15, No 2, 1999.

8. Huang, S.J. and H.C. Chao, "Fuzzy Logic Controller for a Vehicle Active Suspension System", presented at the Proceedings of the Institution of Mechanical Engineers, Part D; Journal of Automobile Engineering, Vol 214, No D1, 2000, pp1-12.

9. Varadi, Peter C., Gwo-Jeng Lo, Oliver M. O'Reilly and Panayiotis Papadopoulos, "A Novel Approach to Vehicle Dynamics Using the Theory of a Cosserat Point and Its Application to Collision Analyses of Platooning Vehicles", *Vehicles System Dynamics*, Vol 32, No 1, July 1999, 99 85-108.

10. Zhang, Yuan, Paul Xiao, Tim Palmer and Akbar Faraham, "Vehicle Chassis/Suspension Dynamics Analysis-Finite Element Model vs. Rigid Body Model", SAE Paper 980900, 1998, pp 113-126.

11. Kawagoe, Kenji, Kenji Suma and Masayuki Watanabe, "Evaluation and Improvement of Vehicle Roll Behavior", SAE Paper 970093 Presented at International Congress and Exposition, Detroit, MI, February 24-27, 1997.

12. Mehrabi, M.G., R.M.H. Cheng and A. Hemami, "Parametric Study and Sensitivity Analysis of Automated Vehicles", *Robotica*, Vol 13, September –October 1995, pp 469-475.

13. El-Demerdash, S.M., "Performance of Limited Bandwith Active Suspension Based on a Half Car Model", SAE Paper 981119, pp 177-186, *Developments in Tire, Wheel, Steering and Suspension Technology*, SP-1338, 1998.

14. Loeb, Jeff S., Dennis A Guenther, Hung-Hsu Fred Chen and John R. Ellis, "Lateral Stiffness, Cornering Stiffness and Relaxation Length of the Pneumatic Tire", SAE Paper 900129, 1990.

15. Chiesa, A. and L. Rinonapoli, "Vehicle Stability Studied with a Non-Linear Seven Degree Model", pp 1708-1724.

16. Taylor, R.K., L.L. Bashford and M.D. Schrock, "Methods for Measuring Vertical Tire Stiffness", Transactions of the ASME, ASME, Vol 43, No 6, November-December 2000, pp 1415-1419.

17. Salaani, Mohamed Kamel, Jeffrey P. Chrstos and Dennis A. Guenther, "Parameter Measurement and Development of a NADSdyna Validation Data Set for a 1994 Ford Taurus", SAE Paper 970564, presented at International Congress and Exposition, Detroit, MI, February 24-27, 1997.

18. Nalecz, Andrej G. and Alan C. Bindemann, "Handling Properties of Four Wheel Steering Vehicles", SAE Paper 890080, 1989.

19. Mousseau, C.W., T.A. Laursen, M. Lidberg and R.L. Taylor, "Vehicle Dynamics Simulations with Coupled Multibody and Finite Element Methods", *Finite Elements in Analysis and Design*, Vol 31, No 4, 1999, pp 295-315.

20. Sekula, P.J., G.L. Hall, G.R. Potts and F.S. Conant, "Dynamic Indoor Tire Testing and Fourier Transform Analysis", *Tire Science and Technology*, Vol 4, No 2, May 1976, pp 66-85.

21. Elbay, S. and Y.M. Ram, "An Affine Inverse Eigenvalue Problem", 2002 (to appear).

APPENDIX: MATLAB PROGRAMS

1. **Program to determine the poles and eigenvectors of a mass-spring-damper system for free vibration.**

```
clear all
kf=225000; in N/m
kr=300000; in N/m
cf=500; in N-s/m
cr=600; in N-s/m
m=2519; in kilograms
l1=2.53; in meters
ig=m*l1^2;
l=2.95; in meters
k1=2*kf; total spring rate for both front tires
k2=2*kr; total spring rate for both rear tires
c1=2*cf; total damping rate for both front tires
c2=2*cr; total damping rate for both rear tires
```

Formulation of M, C, K, A, and B matrices

```
M=[m 0;0 ig];
K=[k1+k2 l/2*(k2-k1);l/2*(k2-k1) l^2/4*(k1+k2)];
C=[c1+c2 l/2*(c2-c1);l/2*(c2-c1) l^2/4*(c1+c2)];
A=[zeros(2,2) eye(2);-K zeros(2,2)];
B=[eye(2) zeros(2,2);C M];
```

Determination and plot of poles and eigenvectors

```
[v,s]=eig(A,B)

figure(1)
plot(s,'.')

v1=v(:,1);
v2=v(:,3);
v3=v(:,2);
v4=v(:,4);

figure(2)
plot(real(v1),'bo-')
hold on;
plot(imag(v1),'k*-')
plot(abs(v1),'rx-')
grid on;
```

```
figure(3)
plot(real(v2),'bo-')
hold on;
plot(imag(v2),'k*-')
plot(abs(v2),'rx-')
grid on;

figure(4)
plot(real(v3),'bo-')
hold on;
plot(imag(v3),'k*-')
plot(abs(v3),'rx-')
grid on;

figure(5)
plot(real(v4),'bo-')
hold on;
plot(imag(v4),'k*-')
plot(abs(v4),'rx-')
grid on;
```

2. **Program to determine poles and eigenvectors of a mass-spring-damper system with an external force.**

```
clear all
kf=225000;
kr=300000;
cf=500;
cr=600;
m=2519;
l1=2.53;
ig=m*l1^2;
l=2.95;
k1=2*kf;
k2=2*kr;
c1=2*cf;
c2=2*cr;
```

Formulation of M, C, K matrices

```
M=[m 0;0 ig];
K=[k1+k2 l/2*(k2-k1);l/2*(k2-k1) l^2/4*(k1+k2)];
C=[c1+c2 l/2*(c2-c1);l/2*(c2-c1) l^2/4*(c1+c2)];
n=100; n represents the maximum time interval in 100th of a second
dw=1/n; dw represents the increment for the natural frequency interval
w=[0:dw:30]';
```

```
[zzz,dum]=size(w);
f=[1;0];
```

Determination of frequency response and phase function

```
for i=1:zzz,
  A=[K-w(i)^2*M w(i)*C;-w(i)*C K-w(i)^2*M];
  B=[zeros(2,1);f];
  sol=inv(A)*B;
  p=sol(1:2,1);
  q=sol(3:4,1);
  X1(i,1)=sqrt(p(1,1)^2+q(1,1)^2);
  F1(i,1)=atan2(q(1,1),p(1,1));
  X2(i,1)=sqrt(p(2,1)^2+q(2,1)^2);
  F2(i,1)=atan2(q(2,1),p(2,1));
end
```

Plot of frequency response and phase function

```
figure(1);
semilogy(w,X1);
grid on;

figure(2);
plot(w,F1);
grid on;

figure(3);
semilogy(w,X2);
grid on;

figure(4);
plot(w,F2);
grid on;
```

3. **Program to determine the natural frequencies when the parameter J is perturbed.**

```
clear all
for ii=1:6,
l1=2.53+(ii-1)*0.1;
kf=225000;
kr=300000;
cf=500;
cr=600;
m=2519;
```

```
ig=m*l1^2;
l=2.95;
k1=2*kf;
k2=2*kr;
c1=2*cf;
c2=2*cr;
```

Formulation of M, C, and K matrices

```
M=[m 0;0 ig];
K=[k1+k2 l/2*(k2-k1);l/2*(k2-k1) l^2/4*(k1+k2)];
C=[c1+c2 l/2*(c2-c1);l/2*(c2-c1) l^2/4*(c1+c2)];
n=1001;
dw=0.025;
w=[0:dw:n*dw]';
[zzz,dum]=size(w);
f=[1;0];
```

Determination of frequency response and phase function

```
for i=1:zzz,
  A=[K-w(i)^2*M w(i)*C;-w(i)*C K-w(i)^2*M];
  B=[zeros(2,1);f];
  sol=inv(A)*B;
  p=sol(1:2,1);
  q=sol(3:4,1);
  X1(i,ii)=sqrt(p(1,1)^2+q(1,1)^2);
  F1(i,ii)=atan2(q(1,1),p(1,1));
  X2(i,ii)=sqrt(p(2,1)^2+q(2,1)^2);
  F2(i,ii)=atan2(q(2,1),p(2,1));
end
end
```

Plot of frequency response and phase function

```
figure(1);
semilogy(w,X1);
grid on;

figure(2);
plot(w,F1);
grid on;

figure(3);
semilogy(w,X2);
grid on;
```

```
figure(4);
plot(w,F2);
grid on;
```

4. Program to determine the natural frequencies when the parameter m is perturbed.

```
clear all
for ii=1:6,
l1=2.53;
kf=225000;
kr=300000;
cf=500;
cr=600;
m=2519+(ii-1)*200;
ig=m*l1^2;
l=2.95;
k1=2*kf;
k2=2*kr;
c1=2*cf;
c2=2*cr;
```

Formulation of M, C, and K matrices

```
M=[m 0;0 ig];
K=[k1+k2 l/2*(k2-k1);l/2*(k2-k1) l^2/4*(k1+k2)];
C=[c1+c2 l/2*(c2-c1);l/2*(c2-c1) l^2/4*(c1+c2)];
n=1001;
dw=0.025;
w=[0:dw:n*dw]';
[zzz,dum]=size(w);
f=[1;0];
```

Determination of frequency response and phase function

```
for i=1:zzz,
  A=[K-w(i)^2*M w(i)*C;-w(i)*C K-w(i)^2*M];
  B=[zeros(2,1);f];
  sol=inv(A)*B;
  p=sol(1:2,1);
  q=sol(3:4,1);
  X1(i,ii)=sqrt(p(1,1)^2+q(1,1)^2);
  F1(i,ii)=atan2(q(1,1),p(1,1));
  X2(i,ii)=sqrt(p(2,1)^2+q(2,1)^2);
  F2(i,ii)=atan2(q(2,1),p(2,1));
```

```
end
end
```

Plot of frequency response and phase function

```
figure(1);
semilogy(w,X1);
grid on;

figure(2);
plot(w,F1);
grid on;

figure(3);
semilogy(w,X2);
grid on;

figure(4);
plot(w,F2);
grid on;
```

5. **Program to determine the natural frequencies when the parameter k_1 is perturbed.**

```
clear all
for ii=1:6,
l1=2.53;
kf=  225000+(ii-1)*2000;
kr=300000;
cf=500;
cr=600;
m=2519;
ig=m*l1^2;
l=2.95;
k1=2*kf;
k2=2*kr;
c1=2*cf;
c2=2*cr;
```

Formulation of M, C, and K matrices

```
M=[m 0;0 ig];
K=[k1+k2 l/2*(k2-k1);l/2*(k2-k1) l^2/4*(k1+k2)];
C=[c1+c2 l/2*(c2-c1);l/2*(c2-c1) l^2/4*(c1+c2)];
n=1001;
```

```
dw=0.025;
w=[0:dw:n*dw]';
[zzz,dum]=size(w);
f=[1;0];
```

Determination of frequency response and phase function

```
for i=1:zzz,
  A=[K-w(i)^2*M w(i)*C;-w(i)*C K-w(i)^2*M];
  B=[zeros(2,1);f];
  sol=inv(A)*B;
  p=sol(1:2,1);
  q=sol(3:4,1);
  X1(i,ii)=sqrt(p(1,1)^2+q(1,1)^2);
  F1(i,ii)=atan2(q(1,1),p(1,1));
  X2(i,ii)=sqrt(p(2,1)^2+q(2,1)^2);
  F2(i,ii)=atan2(q(2,1),p(2,1));
end
end
```

Plot of frequency response and phase function

```
figure(1);
semilogy(w,X1);
grid on;

figure(2);
plot(w,F1);
grid on;

figure(3);
semilogy(w,X2);
grid on;

figure(4);
plot(w,F2);
grid on;
```

6. **Program to determine the natural frequencies when the parameter c_1 is perturbed.**

```
clear all
for ii=1:6,
l1=2.53;
kf=225000;
```

```
kr=300000;
cf=  500+(ii-1)*10;
cr=600;
m=2519;
ig=m*l1^2;
l=2.95;
k1=2*kf;
k2=2*kr;
c1=2*cf;
c2=2*cr;
```

Formulation of M, C, and K matrices

```
M=[m 0;0 ig];
K=[k1+k2 l/2*(k2-k1);l/2*(k2-k1) l^2/4*(k1+k2)];
C=[c1+c2 l/2*(c2-c1);l/2*(c2-c1) l^2/4*(c1+c2)];
n=1001;
dw=0.025;
w=[0:dw:n*dw]';
[zzz,dum]=size(w);
f=[1;0];
```

Determination of frequency response and phase function

```
for i=1:zzz,
  A=[K-w(i)^2*M w(i)*C;-w(i)*C K-w(i)^2*M];
  B=[zeros(2,1);f];
  sol=inv(A)*B;
  p=sol(1:2,1);
  q=sol(3:4,1);
  X1(i,ii)=sqrt(p(1,1)^2+q(1,1)^2);
  F1(i,ii)=atan2(q(1,1),p(1,1));
  X2(i,ii)=sqrt(p(2,1)^2+q(2,1)^2);
  F2(i,ii)=atan2(q(2,1),p(2,1));
end
end
```

Plot of frequency response and phase function

```
figure(1);
semilogy(w,X1);
grid on;

figure(2);
plot(w,F1);
grid on;
```

```
figure(3);
semilogy(w,X2);
grid on;

figure(4);
plot(w,F2);
grid on;
```

7. Program to perform the sensitivity analysis on J for the perturbations in the parametric analysis.

```
clear all;
for ii=1:6,
  l1=2.53+(ii-1)*0.1;
  kf=225000;
  kr=300000;
  cf=500;
  cr=600;
  m=2519;
  ig(ii)=m*l1^2;
  J=ig(ii);
  l=2.95;
  k1=2*kf;
  k2=2*kr;
  c1=2*cf;
  c2=2*cr;
```

Formulation of M, C, and K matrices

```
  M=[m 0;0 J];
  K=[k1+k2 l/2*(k2-k1);l/2*(k2-k1) l^2/4*(k1+k2)];
  C=[c1+c2 l/2*(c2-c1);l/2*(c2-c1) l^2/4*(c1+c2)];

  A=[zeros(2,2) eye(2);-inv(M)*K -inv(M)*C];
  [U,S]=eig(A);
    [s,ind]=sort(diag(S));
  U=U(:,ind);
  V=inv(U');
```

ds_1/dJ

```
  dA_dJ=[zeros(2,4);-[0 0;0 -1/J^2]*K -[0 0;0 -1/J^2]*C];
  y1=V(:,1);
  x1=U(:,1);
  ds1_dJ(ii,1)=y1'*dA_dJ*x1/(y1'*x1);
```

check for s

```
  dJ=0.1;
  M1=[m 0;0 J+dJ];
  A1=[zeros(2,2) eye(2);-inv(M1)*K -inv(M1)*C];
  [U1,S1]=eig(A1);
  [s1,ind]=sort(diag(S1));
  U1=U1(:,ind);
  zz1(ii,1)=(s1(1)-s(1))/dJ;
```

ds_2/dJ

```
  y2=V(:,3);
  x2=U(:,3);
  ds2_dJ(ii,1)=y2'*dA_dJ*x2/(y2'*x2);
```

check for s

```
  zz2(ii,1)=(s1(3)-s(3))/dJ;
end
[ds1_dJ zz1]
[ds2_dJ zz2]

figure(1)
plot(ig,[real(ds1_dJ),real(ds2_dJ)])
grid on;
figure(2)
plot(ig,[imag(ds1_dJ),imag(ds2_dJ)])
grid on;
```

8. **Program to perform the sensitivity analysis on m for the perturbations in the parametric analysis.**

```
clear all;
for ii=1:6,
  l1=2.53;
  kf=225000;
  kr=300000;
  cf=500;
  cr=600;
  m=  2519+(ii-1)*200;
  ig(ii)=m*l1^2;
  J=ig(ii);
  l=2.95;
  k1=2*kf;
```

```
k2=2*kr;
c1=2*cf;
c2=2*cr;
```

Formulation of M, C, and K matrices

```
M=[m 0;0 J];
K=[k1+k2 l/2*(k2-k1);l/2*(k2-k1) l^2/4*(k1+k2)];
C=[c1+c2 l/2*(c2-c1);l/2*(c2-c1) l^2/4*(c1+c2)];

A=[zeros(2,2) eye(2);-inv(M)*K -inv(M)*C];
[U,S]=eig(A);
  [s,ind]=sort(diag(S));
U=U(:,ind);
V=inv(U');
```

ds_1/dJ

```
dA_dm=[zeros(2,4);-[-1/m^2 0;0 -r^2/J^2]*K -[-1/m^2 0;0 -r^2/J^2]*C];
y1=V(:,1);
x1=U(:,1);
ds1_dm(ii,1)=y1'*dA_dm*x1/(y1'*x1);
```

check for s

```
dm=0.1;
M1=[m+dm 0;0 (m+dm)*l1^2];
A1=[zeros(2,2) eye(2);-inv(M1)*K -inv(M1)*C];
[U1,S1]=eig(A1);
[s1,ind]=sort(diag(S1));
U1=U1(:,ind);
zz1(ii,1)=(s1(1)-s(1))/dm;
```

ds_2/dJ

```
y2=V(:,3);
x2=U(:,3);
ds2_dm(ii,1)=y2'*dA_dm*x2/(y2'*x2);
```

check for s

```
  zz2(ii,1)=(s1(3)-s(3))/dm;
end
[ds1_dm zz1]
[ds2_dm zz2]

figure(1)
```

```
plot(ig,[real(ds1_dm),real(ds2_dm)])
grid on;
figure(2)
plot(ig,[imag(ds1_dm),imag(ds2_dm)])
grid on;
```

9. Program to perform the sensitivity analysis on k_1 for the perturbations in the parametric analysis.

```
clear all;
for ii=1:6,
  l1=2.53;
  kf=  225000+(ii-1)*2000;
  kr=300000;
  cf=500;
  cr=600;
  m=2519;
  ig(ii)=m*l1^2;
  J=ig(ii);
  l=2.95;
  k1=2*kf;
  k2=2*kr;
  c1=2*cf;
  c2=2*cr;
```

Formulation of M, C, and K matrices

```
  M=[m 0;0 J];
  K=[k1+k2 l/2*(k2-k1);l/2*(k2-k1) l^2/4*(k1+k2)];
  C=[c1+c2 l/2*(c2-c1);l/2*(c2-c1) l^2/4*(c1+c2)];

  A=[zeros(2,2) eye(2);-inv(M)*K -inv(M)*C];
  [U,S]=eig(A);
    [s,ind]=sort(diag(S));
  U=U(:,ind);
  V=inv(U');
```

$ds_1/dk1$:

```
  dA_dk1=[zeros(2,4);-inv(M)*[1 -l/2;-l/2 l^2/4] zeros(2,2)];
  y1=V(:,1);
  x1=U(:,1);
  ds1_dk1(ii,1)=y1'*dA_dk1*x1/(y1'*x1);
```

check for s

```
  dk1=0.1;
  K1=[k1+k2+dk1 l/2*(k2-k1-dk1);l/2*(k2-k1-dk1) l^2/4*(k1+k2+dk1)];
  A1=[zeros(2,2) eye(2);-inv(M)*K1 -inv(M)*C];
  [U1,S1]=eig(A1);
  [s1,ind]=sort(diag(S1));
  U1=U1(:,ind);
  zz1(ii,1)=(s1(1)-s(1))/dk1;
```

ds_2/dk_1

```
  y2=V(:,3);
  x2=U(:,3);
  ds2_dk1(ii,1)=y2'*dA_dk1*x2/(y2'*x2);
```

check for s

```
  zz2(ii,1)=(s1(3)-s(3))/dk1;
end
[ds1_dk1 zz1]
[ds2_dk1 zz2]

figure(1)
plot(ig,[real(ds1_dk1),real(ds2_dk1)])
grid on;
figure(2)
plot(ig,[imag(ds1_dk1),imag(ds2_dk1)])
grid on;
```

10. Program to perform the sensitivity analysis on c_1 for the perturbations in the parametric analysis.

```
clear all;
for ii=1:6,
  l1=2.53;
  kf=225000;
  kr=300000;
  cf=500  500+(ii-1)*10;
  cr=600;
  m=2519;
  damp(ii)=c1;
  J=ig(ii);
  l=2.95;
  k1=2*kf;
  k2=2*kr;
  c1=2*cf;
```

```
c2=2*cr;
```

Formulation of M, C, and K matrices

```
M=[m 0;0 J];
K=[k1+k2 l/2*(k2-k1);l/2*(k2-k1) l^2/4*(k1+k2)];
C=[c1+c2 l/2*(c2-c1);l/2*(c2-c1) l^2/4*(c1+c2)];

A=[zeros(2,2) eye(2);-inv(M)*K -inv(M)*C];
[U,S]=eig(A);
  [s,ind]=sort(diag(S));
U=U(:,ind);
V=inv(U');
```

ds_1/dc_1

```
dA_dc1=[zeros(2,4);zeros(2,2) -inv(M)*[1 -l/2;-l/2 l^2/4]];
y1=V(:,1);
x1=U(:,1);
ds1_dc1(ii,1)=y1'*dA_dc1*x1/(y1'*x1);
```

check for s

```
dc1=0.1;
C1=[c1+c2+dc1 l/2*(c2-c1-dc1);l/2*(c2-c1-dc1) l^2/4*(c1+c2+dc1)];
A1=[zeros(2,2) eye(2);-inv(M)*K -inv(M)*C1];
[U1,S1]=eig(A1);
[s1,ind]=sort(diag(S1));
U1=U1(:,ind);
zz1(ii,1)=(s1(1)-s(1))/dc1;
```

ds_2/dJ: Sensitivity on J

```
y2=V(:,3);
x2=U(:,3);
ds2_dc1(ii,1)=y2'*dA_dJ*x2/(y2'*x2);
```

check for s

```
  zz2(ii,1)=(s1(3)-s(3))/dc1;
end
[ds1_dc1 zz1]
[ds2_dc1 zz2]

figure(1)
plot(ig,[real(ds1_dc1),real(ds2_dc1)])
grid on;
```

```
figure(2)
plot(ig,[imag(ds1_dc1),imag(ds2_dc1)])
grid on;
```

11. Program to calculate natural frequencies for free vibration for experiment-base system.

```
clear all
b=0.36;
k1=2540;
m=1.569;
J=1/12*m*b^2;
l=b;

M=[m 0;0 J];
K=[4*k1 0;0 l^2*k1];

[v,s]=eig(K,M)
```

12 Program to calculate natural frequencies for free vibration for experiment with added mass.

```
clear all
m1=[0.063;0.122];
for ii=1:2,
  b=0.36;
  k1=2540;
  m=1.569+m1(ii);
  J=1/12*m*b^2;
  l=b;
  M=[m 0;0 J];
  K=[4*k1+k3(ii) 0;0 l^2*k1];
  [v,s]=eig(K,M)
end
```

13. Program to calculate natural frequencies for free vibration for experiment with center spring.

```
clear all
k3=[910.7;1313];
for ii=1:2,
  b=0.36;
  k1=2540;
  m=1.569;
  J=1/12*m*b^2;
```

```
  l=b;
  M=[m 0;0 J];
  K=[4*k1+k3(ii) 0;0 l^2*k1];
  [v,s]=eig(K,M)
end
```

14. Program to calculate the sensitivity analysis for mass perturbations for experimental setup.

```
clear all
mm=[0.063;0.122];
for ii=1:2,
  b=0.36;
  k1=2540;
  m=1.569+mm(ii);
  J=1/12*m*b^2;
  l=b;% in meters
  M=[m 0;0 J];
  K=[4*k1 0;0 l^2*k1];
  C=[0 0;0 0];
  mass(ii)=m;

  A=[zeros(2,2) eye(2);-inv(M)*K -inv(M)*C];
  [U,S]=eig(A);
  [s,ind]=sort(diag(S));
  U=U(:,ind);
  V=inv(U');
```

¶s₁/¶m

```
  dA_dm=[zeros(2,4);[-1/m^2 0;0 -12/(m^2*b^2)]*K zeros(2,2)];
  y1=V(:,1);
  x1=U(:,1);
  ds1_dm(ii,1)=y1'*dA_dm*x1/(y1'*x1);
```

check for s

```
  dm=0.001;
  M1=[m+dm 0;0 (m+dm)*b^2/12];
  A1=[zeros(2,2) eye(2);-inv(M1)*K -inv(M)*C];
  [U1,S1]=eig(A1);
  [s1,ind]=sort(diag(S1));
  U1=U1(:,ind);
  zz1(ii,1)=(s(1)-s1(1))/dm;
```

$\P s_2 / \P m$

```
  y2=V(:,3);
  x2=U(:,3);
  ds2_dm(ii,1)=y2'*dA_dm*x2/(y2'*x2);
```

check for s

```
  zz2(ii,1)=(s(3)-s1(3))/dm;
end
[ds1_dm zz1]
[ds2_dm zz2]

figure(1)
plot(mass,[real(ds1_dm),real(ds2_dm)])
grid on;
figure(2)
plot(mass,[imag(ds1_dm),imag(ds2_dm)])
grid on;
```

15 Program to calculate the sensitivity for the perturbations in the stiffness for the free vibration.

```
clear all
k3=[910.7;1313];
for ii=1:2,
  b=0.36;
  k1=2540;
  m=1.569;
  J=1/12*m*b^2;
  l=b;
  M=[m 0;0 J];
  K=[4*k1+k3(ii) 0;0 l^2*k1];
  C=[0 0;0 0];
  stiff(ii)=k3(ii);

  A=[zeros(2,2) eye(2);-inv(M)*K -inv(M)*C];
  [U,S]=eig(A);
  [s,ind]=sort(diag(S));
  U=U(:,ind);
  V=inv(U');
```

$\P s_1 / \P k_1$

```
  dA_dk1=[zeros(2,4);-inv(M)*[1 0;0 0] zeros(2,2)];
  y1=V(:,1);
```

```
  x1=U(:,1);
  ds1_dk1(ii,1)=y1'*dA_dk1*x1/(y1'*x1);

                                        check for s
  dk3=0.1;
  K1=[4*k1+k3(ii)+dk3 0;0 l^2*k1];
  A1=[zeros(2,2) eye(2);-inv(M)*K1 -inv(M)*C];
  [U1,S1]=eig(A1);
  [s1,ind]=sort(diag(S1));
  U1=U1(:,ind);
  zz1(ii,1)=(s1(1)-s(1))/dk3;

                                        ¶s2/ ¶k3

  y2=V(:,3);
  x2=U(:,3);
  ds2_dk1(ii,1)=y2'*dA_dk1*x2/(y2'*x2);

                                        check for s
  zz2(ii,1)=(s1(3)-s(3))/dk3;
end
[ds1_dk1 zz1]
[ds2_dk1 zz2]

figure(1)
plot(stiff,[real(ds1_dk1),real(ds2_dk1)])
grid on;
figure(2)
plot(stiff,[imag(ds1_dk1),imag(ds2_dk1)])
grid on;
```

VITA

Kanika Nicole Vessel was born on March 7, 1977, in Detroit, Michigan, to Theophilus and Nordica Mixon, Jr. She went to high school in Detroit, Michigan at Martin Luther King, Jr. High School. She obtained a Bachelor of Science in Mechanical Engineering from Southern University and A & M College in Baton Rouge, Louisiana. Following graduation, she decided to pursue a graduate degree in mechanical engineering at Louisiana State University-Baton Rouge, Louisiana, with specialization in mechanical systems and vibration. She successfully defended her thesis on Friday, April 12, 2002, and will be graduating with a Master of Science degree in Mechanical Engineering in May 2002. She will continue to pursue a doctoral degree in engineering science at Louisiana State University-Baton Rouge, Louisiana. Currently, she is taking classes that will fulfill part of her requirements to obtain a Doctor of Philosophy degree.